Graphical evaluation of relativistic matrix elements*

Keh-Ning Huang

Behlen Laboratory of Physics, University of Nebraska, Lincoln, Nebraska 68588

A graphical representation of angular momentum is used to evaluate relativistic matrix elements between antisymmetrized states of many- particle configurations having any number of open shells. The antisymmetrized matrix element is expanded as a sum of semisymmetrized matrix elements, which can be evaluated expediently in terms of radial integrals from easily constructed diagrams. The diagram representing a semisymmetrized matrix element is composed of four diagram blocks, namely, the bra block, the ket block, the spectator block, and the interaction block. The first three blocks indicate the couplings of the two interacting configurations while the last depends on the interaction and is the replaceable component. Interaction blocks for relativistic operators and commonly used potentials are summarized in ready-to-use forms. A simple step-by-step procedure is prescribed generally for calculating antisymmetrized matrix elements of one- and two-particle operators. A modified covarient 3-jm coeffecient is also introduced along with certain new graphical notations. Although we focus on the case of jj-coupled states, which comes naturally in relativistic formulation, the general procedure holds in any coupling scheme.

CONTENTS

*Present address: Department of Physics, University of Notre Dame, Notre Dame, Indiana 46556.

I. INTRODUCTION

A relativistic treatment including correlation and quantum-electrodynamic corrections has become essential in many fields of atomic physics; this requires the evaluation of matrix elements with considerable complexity. In particular, the possibility of forming highly ionized heavy atoms and the study of their structure and of their collision and subsequent cascade processes necessitate a complete treatment of couplings between several open shells. On the other hand, the application of standard techniques of angular momentum coupling in these problems becomes a tedious and more often arduous task. The purpose of this work is to provide nonspecialists with a simple and powerful tool to express complicated matrix elements in terms of radial integrals, suitable for numerical computation.

One of the essential approximations in the quantum-mechanical description of a many-particle system is the central field approximation. Orbitals of the particles can thus be represented by angular-momentum eigenstates. The coupling of angular-momentum eigenstates with irreducible tensor operators depends only on the rotational properties of the states and operators involved. This fact leads naturally to the division of the calculation of a physical quantity into two parts: One consists of dynamical variables invariant under rotations, and the other is a geometrical factor depending on the rotational properties of the physical quantity. It is the Wigner–Eckart theorem (Wigner, 1927; Eckart, 1930) which embodies this notion. The geometrical factor is given by the *Clebsch-Gordan coefficient* (also called the *Wigner*

or *vector-coupling coefficient)* or by a more symmetric quantity, *the Wigner 3-j coefficient* (Wigner, 1951; Edmonds, 1957). Techniques for the solution of related algebraic problems for many-particle systems have been developed by Racah (1942a, 1942b, 1943). [Two other equally applicable approaches have been described in the works of Condon and Shortley (1935) and Harter and Patterson (1976), respectively, but will not be discussed here.] However, the complicated algebraic manipulations have prevented nonspecialists from carrying out specific calculations.

Attempts to solve the complexity of angular momentum couplings result in graphical methods. In the early stage, angular momentum diagrams were used only in a qualitative and descriptive way (see, e.g., Edmonds, 1957, and Judd, 1963). It was the achievement of Jucys, Levinson, and Vanagas (1962) that a graphical method was put on a quantitative basis so that angular momentum couplings can be solved in an expedient and elegant manner solely in terms of diagrams. The graphical method of Jucys *et al.* starts by assigning a graphical symbol to the Wigner 3-*j* coefficient and compounds the angular momentum coupling to *3n-j symbols*. An alternative method given by Danos (1971), however, focuses on the recoupling aspect and uses the 9-*j* recoupling as the central graphical element. The former has been particularly effective in extending the range of application of Racah's techniques. The graphical approach permits transformations on diagrammatic expressions and leads on to analytical results in a clear and simple manner. Besides its utility as a calculational tool, the graphical method has the appealing feature of revealing, at a glance, the structure of very complicated couplings of angular momenta. In addition, we do gain in the graphical form some physical insight, similar to the visual understanding of physical processes provided by Feynman diagrams. In fact, because of the role which the graphical method plays in extracting the geometrical part of a Feynman diagram (Bolotin, Levinson, and Tolmacher, 1964; Judd, 1967; El-Baz and Nahabetian, 1969), it becomes an indispensable supplement to the Feynman diagrams, where a perturbed quantum-mechanical system is studied graphically.

The graphical method has been developed subsequently by Jucys and Bandzaitis (1967), Massot, El-Baz, and Lafoucriere (1967), Brink and Satchler (1968), El-Baz (1969), Sandars (1969), Bordarier (1970), Briggs (1971), and El-Baz and Castel (1971, 1972). El-Baz and co-workers have in particular extended the graphical method to treat spherical harmonics, irreducible tensors, and rotation matrices. The basic idea of El-Baz and Castel (1972) consists in introducing graphical symbols for the bra (covariant) and ket (contravariant) vectors familiar in the Dirac notations (Dirac, 1930). The graphical representation of the Clebsh-Gordan coefficient thus becomes a straightforward extension of the bra and ket diagrams. The graphical representation of the Wigner 3-*j* coefficient, first introduced by Jucys *et al.* (1962), has been modified by El-Baz (1969) to better represent its covariant property, using Wigner's covariant notation (Wigner, 1959). We will adopt this idea of El-Baz with a modified phase factor to have a more coherent correspondence between the Wigner 3-*j* coefficient and the Clebsch-Gordan coefficient.

A graphical treatment of antisymmetrization for the evaluation of antisymmetrized matrix elements has been given by Bordarier (1970) and Briggs (1971). Bordarier's treatment is general and encompasses many different types of matrix elements, while Briggs using a similar approach gives a step-by-step procedure for the evaluation of matrix elements of spin-independent operators in the *LS* coupling. An alternative treatment has been given by Huang and Starace (1978) for a particular case. The procedure of Bordarier and Briggs is, however, a little intricate between purely graphical steps and manipulations which are better performed analytically. For example, the antisymmetrization of particles from different subshells may be carried out analytically with ease without resorting to a graphical phase rule. Furthermore, the interaction diagram is obtained in the Briggs' prescription by expanding the interaction operator in a complete set of particle orbitals, whereas a similar interaction diagram may be obtained by considering directly the *m*-scheme matrix element.

In this work, we will prescribe a simple step-by-step procedure for evaluating antisymmetrized matrix elements for one- and two-particle operators. Although we focus on the case of *jj*-coupled states, which comes naturally in a relativistic formulation, the general procedure holds in any coupling scheme. The underlying idea of the present approach is to express analytically the matrix element between *antisymmetrized many-particle states* in terms of matrix elements between *semisymmetrized many-particle states*. The semisymmetrized many-particle state is defined as the many-particle state which is antisymmetric within each subshell but is not antisymmetric with respect to exchange of two particles from different subshells. Henceforth, the matrix elements between semisymmetrized many-particle states are evaluated by a graphical procedure. The graphical procedure consists of three major steps: First, we construct diagrams for the two interacting semisymmetrized many-particle states and decouple *active particles* from the other particles to be referred to as *the spectator particles*. Here the active particles represent the typical particles which actually participate in the interaction in a semisymmetrized matrix element. Second, we insert *the interaction block* corresponding to the interaction between active particles. The interaction blocks for commonly used operators and potentials are summarized in ready-to-use forms in Appendix B. Last, we evaluate the resultant diagram by factoring it into basic diagrams representing 3*n*-*j* symbols, for which analytical values have been tabulated extensively (Rotenberg *et al.*, 1959; Jucys *et al.*, 1962). Thus the antisymmetrized matrix element is expressed as a sum of weighted radial integrals.

The graphical notation and transformation rules used in this work are given in Sec. II. The *covariant 3-jm coefficient* is defined there. In Sec. III an analytical procedure is outlined for evaluating the antisymmetrized matrix element in terms of radial integrals. In Sec. IV we describe in detail how the diagram representing the semisymmetrized matrix element can be constructed and evaluated. In Sec. V we summarize the procedure

of evaluating antisymmetrized matrix elements. A worked example is given in Sec. VI. Appendix A is a glossary of definitions of terms used in this work; in most cases they are identified in the text by italic letters when they first appear. Graphical forms of commonly used operators and potentials are summarized in Appendix B. Appendix C gives the derivation of one of the expansion formulas used in Appendix B.

II. GRAPHICAL NOTATION AND TRANSFORMATION RULES

We first define angular momentum bra and ket states and introduce their graphical representations in Sec. II.A. The coupling of two angular momentum eigenstates gives rise to *the Clebsch-Gordan coefficient*. The graphical representation of the Clebsch–Gordan coefficient is presented in Sec. II.B. In Sec. II.C, we define the symmetrized *covariant 3-jm coefficient* and give its graphical representation. There the transformation from a Clebsch-Gordan diagram to a 3-jm diagram is also described. Rules to transform the combined 3-jm diagram are given in Sec. II.D. Section II.E summarizes some basic diagrams with their analytical values.

A. Bra and ket states

In the central field approximation, states of a quantum-mechanical system can conveniently be described by angular momentum eigenstates. Let $|jm\rangle$ denote the ket (contravariant) state which is the angular momentum eigenstate of both $\mathbf{J}^2$ and J_z, i.e.,

$$\mathbf{J}^2|jm\rangle = j(j+1)|jm\rangle ,$$

$$J_z|jm\rangle = m|jm\rangle . \tag{2.1}$$

The bra (covariant) conjugate to the ket state $|jm\rangle$ is denoted by $\langle jm|$. The angular momentum eigenstates $|jm\rangle$ form a complete orthonormal set and satisfy the following orthonormality and closure relations.

$$\langle jm|j'm'\rangle = \delta_{jj'}\delta_{mm'} , \tag{2.2}$$

$$\sum_{jm} |jm\rangle\langle jm| = 1 . \tag{2.3}$$

We note, however, that a complete description of a state cannot be given in terms of the angular momentum quantum numbers alone. In what follows, we shall not concern ourselves with these further observables because they are supposed to commute with the angular momentum operators.

We now consider the quantum-mechanical system whose angular momentum $\mathbf{J}$ is the sum of two independent angular momenta $\mathbf{J}_1$ and $\mathbf{J}_2$. The angular momentum eigenstates of $(\mathbf{J}_1^2 J_{1z})$ and $(\mathbf{J}_2^2 J_{2z})$ are denoted by $|j_1 m_1\rangle$ and $|j_2 m_2\rangle$, respectively; they satisfy similar relations as (2.2) and (2.3). The Hilbert space spanned by $|jm\rangle \equiv |(j_1 j_2)jm\rangle$ can also be spanned by $|j_1 m_1 j_2 m_2\rangle \equiv |j_1 m_1\rangle\,|j_2 m_2\rangle$. By using the projection operator

$$\sum_{m_1 m_2} |j_1 m_1 j_2 m_2\rangle\langle j_1 m_1 j_2 m_2| = 1_{j_1 j_2} , \tag{2.4}$$

where $1_{j_1 j_2}$ is the unit operator in the $j_1 j_2$ subspace and zero outside, we can therefore write $|jm\rangle$ in terms of $|j_1 m_1 j_2 m_2\rangle$ as

$$|jm\rangle = \sum_{m_1 m_2} |j_1 m_1 j_2 m_2\rangle\langle j_1 m_1 j_2 m_2|jm\rangle . \tag{2.5}$$

Here the matrix elements $\langle j_1 m_1 j_2 m_2|jm\rangle$ effect the transformation between $|jm\rangle$ and $|j_1 m_1 j_2 m_2\rangle$ and are called *Clebsch–Gordan, Wigner,* or *vector-coupling coefficients* (Rose, 1957; Edmonds, 1957; Fano and Racah, 1959).

Graphically we represent a ket (contravariant) state by a vertical bar with an outgoing arrow, and a bra (covariant) state by a vertical bar with an ingoing arrow,

$|jm\rangle =$ 

,

$\langle jm| =$ 

. (2.6)

This notational rule is different from that employed by El-Baz and Castel (1972). They use a single outgoing arrow to denote a ket state and a double ingoing arrow to denote a bra state, and a reverse in the direction of an arrow indicates a sign change of the magnetic quantum number in the corresponding state. In our notation, we can present the orthonormality and closure relations of angular-momentum eigenstates as

$\langle jm|j'm'\rangle =$ 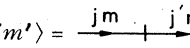

$= \delta_{jj'}\delta_{mm'}$ (2.7)

$\sum_{jm} |jm\rangle\langle jm| = \sum_{jm}$ 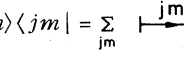

$= \sum_{j}$ 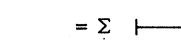

$= 1$, (2.8)

where the summation over the magnetic quantum number m is carried out graphically by joining the contravariant and covariant angular momentum lines to form a single-arrowed line. Similarly the projection operator in (2.4) can be represented as

$\sum_{m_1 m_2} |j_1 m_1 j_2 m_2\rangle\langle j_1 m_1 j_2 m_2| =$ 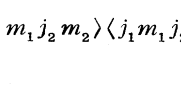

$= 1_{j_1 j_2}$. (2.9)

Hence we can write the expansion (2.5) graphically as

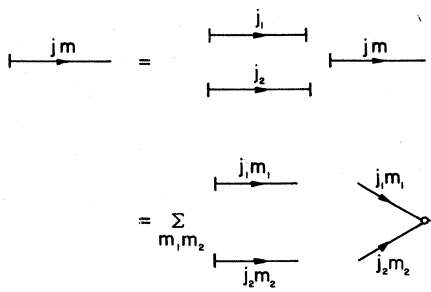

, (2.10)

where the last diagram represents a Clebsch–Gordan coefficient within a phase factor. The graphical representation of the Clebsch–Gordan coefficient thus becomes a straightforward extension of the bra and ket

diagrams (El-Baz, 1969). Furthermore, the phase factor of the Clebsch–Gordan coefficient can also be defined unambiguously by adopting a graphical sign convention; this will be given in the next subsection.

B. The Clebsch-Gordan coefficient

In constructing coupled angular momentum states, where the Clebsch–Gordan coefficient (to be referred to as the C–G coefficient) occurs naturally, one finds that the graphical representation of the C–G coefficient is expedient to use. A graphical representation (El-Baz, 1969) of the C–G coefficient is given by

$$\langle j_1 m_1 j_2 m_2 | j_3 m_3 \rangle = \quad . \tag{2.11}$$

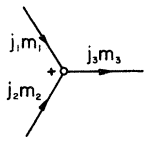

The notational rules are as follows:

(i) Each vertex indicated by a circle represents a C–G coefficient. Each covariant component is denoted by a line with an ingoing arrow, and each contravariant component by a line with an outgoing arrow. In labeling an angular momentum line, the magnetic quantum number is usually suppressed where no confusion may occur.

(ii) The plus (minus) sign at the vertex means that the angular momenta are to be read counterclockwise (clockwise). The change of the sign at the vertex $(j_1 j_2 j_3)$ introduces a phase factor $(-)^{j_1+j_2-j_3}$.

As in (2.8), the summation over a pair of magnetic quantum numbers is performed graphically by joining the corresponding contravariant and covariant angular momentum lines to form a single-arrowed line. Although transformation rules for C–G diagrams have been given (El-Baz and Castel, 1972), we will not present them here because we will use the graphical representation of the C–G coefficient only in constructing many-particle states.

Because C–G coefficients are components of mixed tensors, they are asymmetric when the roles of the participating angular momenta are interchanged. A more symmetric quantity can, however, be obtained by performing an operation corresponding to raising and lowering of indices in tensor algebra. This will be considered in the following section.

C. The covariant 3-*jm* coefficient

The maximum symmetry of a vector-coupling coefficient is obtained in *the Wigner 3-j coefficient* or *symbol* (Wigner, 1951) which is defined by

$$\begin{pmatrix} j_1 & j_2 & j_3 \\ m_1 & m_2 & -m_3 \end{pmatrix} = (-)^{j_1-j_2+m_3}(2j_3+1)^{-1/2}\langle j_1 m_1 j_2 m_2 | j_3 m_3\rangle,$$

where the contravariant component $|j_3 m_3\rangle$ in the C–G coefficient is raised to become a covariant component. Nevertheless, there are advantages in keeping the variance of the components in a C–G coefficient; this can be accomplished by introducing the concept of covariant and contravariant components (Herring, cited in Wigner, 1959) of the Wigner 3-j coefficient. In the covariant notation (Wigner, 1959), *the covariant 3-jm coefficient* (or, simply, *the 3-jm coefficient)* which is, e.g., covariant in the first two indices and contravariant in the last index, is defined by

$$\begin{pmatrix} j_1 & j_2 & m_3 \\ m_1 & m_2 & j_3 \end{pmatrix} = (-)^{j_3+m_3} \begin{pmatrix} j_1 & j_2 & j_3 \\ m_1 & m_2 & -m_3 \end{pmatrix}$$
$$= (-)^{j_1-j_2-j_3}(2j_3+1)^{-1/2}\langle j_1 m_1 j_2 m_2 | j_3 m_3\rangle . \tag{2.12}$$

We emphasize that each component in a 3-jm coefficient is to be treated independently in changing its variance, i.e.,

$$\text{Contravariant: } \begin{pmatrix} m \\ j \end{pmatrix} = (-)^{j+m}\begin{pmatrix} j \\ -m \end{pmatrix},$$
$$\text{Covariant: } \begin{pmatrix} j \\ m \end{pmatrix} = (-)^{j-m}\begin{pmatrix} -m \\ j \end{pmatrix}, \tag{2.13}$$

where (jm) can be any one of the three components in a 3-jm coefficient. Note that this definition differs from Wigner's (Wigner, 1959) in that he used a different phase factor. Our definition conforms with the definition that the Hermitian (covariant) conjugate of a contravariant tensor operator T_{jm} is defined as

$$T^{\dagger}_{jm} = (-)^{j-m} T_{j-m} . \tag{2.14}$$

This choice of phase makes an improvement on the notation for the Wigner–Eckart theorem (Wigner, 1927; Eckart, 1930). [See (3.17) in Sec. III. C and the discussion which follows.] The definition (2.13) also differs from the definition of El-Baz and Castel (1972) in that our contravariant component is defined with the same phase as their covariant component. This modification, however, does not change the graphical transformation rules presented in their work. We also emphasize that the vector-coupling coefficient defined in (2.12) is called "the covariant 3-jm coefficient" because of their covariance properties and m dependence. Accordingly the name "3-j symbol" or "3-j coefficient" will be reserved for the coefficient occurring in the hierarchy of $3n$-j coefficients, which have no m dependence. Definitions of $3n$-j coefficients will be given in Sec. II. E.

By our definition, the Wigner 3-j coefficient is a fully covariant 3-jm coefficient and is equivalent to the fully contravariant 3-jm coefficient

$$\begin{pmatrix} j_1 & j_2 & j_3 \\ m_1 & m_2 & m_3 \end{pmatrix} = \begin{pmatrix} m_1 & m_2 & m_3 \\ j_1 & j_2 & j_3 \end{pmatrix}. \tag{2.15}$$

Note, however, that

$$\begin{pmatrix} j_1 & j_2 & m_3 \\ m_1 & m_2 & j_3 \end{pmatrix} = (-)^{2j_3}\begin{pmatrix} m_1 & m_2 & j_3 \\ j_1 & j_2 & m_3 \end{pmatrix}. \tag{2.16}$$

Graphically we can present a 3-jm coefficient as

$$\begin{pmatrix} j_1 & j_2 & m_3 \\ m_1 & m_2 & j_3 \end{pmatrix} = \quad . \tag{2.17}$$

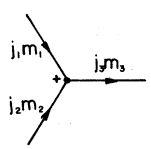

The notational rules are as follows:

(i) Each vertex indicated by a node represents a 3-jm coefficient. Each covariant component is denoted by a line with an ingoing arrow, and each contravariant component by a line with an outgoing arrow. In labeling an angular momentum line, the magnetic quantum number is usually suppressed where no confusion may occur.

(ii) The plus (minus) sign at the node means that the angular momenta are to be read counterclockwise (clockwise). The change of the sign at the node $(j_1 j_2 j_3)$ introduces a phase factor $(-)^{j_1+j_2+j_3}$; therefore the sign at the node may be suppressed if $(j_1+j_2+j_3)$ is an even number. With these notational rules, other examples of 3-jm diagrams are given by

$$\begin{pmatrix} j_1 & m_2 & m_3 \\ m_1 & j_2 & j_3 \end{pmatrix} =$$

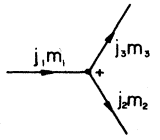

,

$$\begin{pmatrix} j_1 & j_2 & j_3 \\ m_1 & m_2 & m_3 \end{pmatrix} =$$

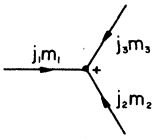

.

We note that the "current" of magnetic quantum numbers is conserved at each node due to the selection rule for magnetic quantum numbers of the 3-jm coefficient; for example,

$$\begin{pmatrix} j_1 & j_2 & m_1+m_2 \\ m_1 & m_2 & j_3 \end{pmatrix} =$$

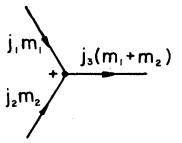

, (2.18)

where we have the sum of the ingoing currents "m_1" +"m_2" = the outgoing current "m_1+m_2."

The notational rules for joining angular momentum lines are as follows:

(i) The summation (or in the tensorial term "contraction") over a pair of magnetic quantum numbers, *one of which is always contravariant, and the other covariant,* is performed by joining the corresponding angular momentum lines to form a linked single-arrowed line.

(ii) The change in direction of a linked angular momentum line j introduces a phase factor $(-)^{2j}$. As a result, we can suppress the arrow of a linked angular momentum line j whenever j is an integer.

Although we do not write the magnetic quantum number for a linked line, the summation over the magnetic quantum number is always implied. Nevertheless, in many cases because of the conservation of the "magnetic current," the summation implied by a linked line exists only formally.

In this work, we will use C–G diagrams to construct many-particle states. The resulting C–G diagrams will then be transformed into 3-jm diagrams by a simple procedure. To transform a C–G diagram into a 3-jm diagram, we do the following:

(i) Add a bar, $\bar{j}$, on the angular momentum j which is unique in its variance character. The bar represents a multiplication factor $(2j+1)^{1/2}$.

(ii) The second (third) angular momentum k, counting from $\bar{j}$ in the direction indicated by the sign of the C–G diagram, introduces a phase factor $(-)^{2k}$ if j is contravariant (covariant). We write a circle around the arrow of the angular momentum line k to denote this phase factor. When the angular momentum line k is joined to another angular momentum line to form a linked line, the circle representing the phase factor $(-)^{2k}$ simply changes the direction of the linked angular momentum line k.

(iii) Fill the vertex into a solid node and change the sign at the node.

Examples of such transformations are

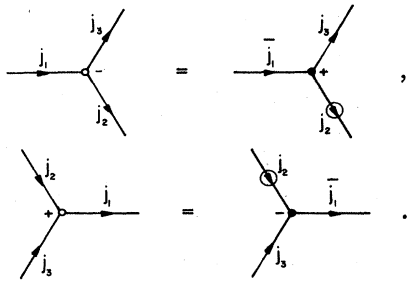

(2.19)

An easy way to remember which angular momentum line k introduces a phase factor $(-)^{2k}$ is that the + (−) sign in the C–G diagram indicates the upper (lower) angular momentum line is to be assigned the phase factor when the diagram is oriented as in (2.19). It is obvious that this phase factor can be omitted when k is an integer. Note the special case

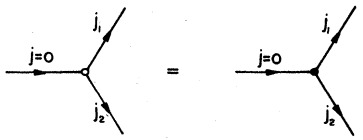

(2.20)

with the sign at the vertex unchanged. Similarly, we have the equivalence

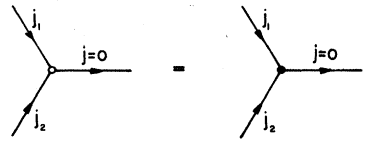

(2.21)

We will find frequent uses of these simple relations in constructing many-particle states.

D. Transformation rules for 3-*jm* diagrams

Transformation rules allow one to manipulate the combined 3-jm diagram. There are only two fundamental transformation rules.

Rule I:

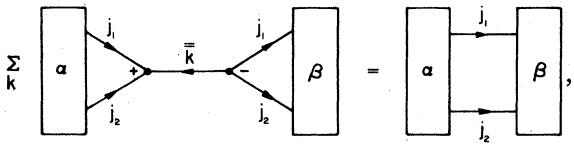

(2.22)

where a bar on the angular momentum $\bar{k}$ stands for a multiplication factor $(2k+1)^{1/2}$, and multiple bars for multiple factors. For example, $\bar{\bar{k}}$ indicates a factor $(2k+1)$. In (2.22) we use the blocks α and β to represent arbitrary diagrams, either open or closed. By *open* or *closed*, we mean that the diagram either has or hasn't any free nonzero angular momentum lines. For example, in the following diagram

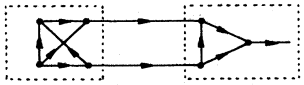

(2.23)

the diagram block on the left is closed while the one on the right is open. We will use an encircled Greek letter @ to indicate specifically a closed diagram block.

Rule I follows from the graphical relation for 3-jm coefficients,

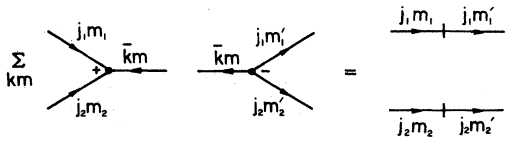

(2.24)

which represents the orthogonality relation

$$\sum_{km}(2k+1)\begin{pmatrix} j_1 & j_2 & k \\ m_1 & m_2 & m \end{pmatrix}\begin{pmatrix} j_1 & j_2 & k \\ m_1' & m_2' & m \end{pmatrix} = \delta_{m_1 m_1'}\,\delta_{m_2 m_2'}\,. \tag{2.25}$$

Rule II:

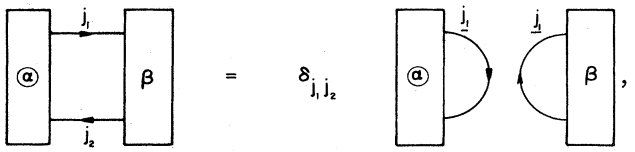

(2.26)

where the right-hand side represents the product of the two adjacent unconnected diagrams. Here the bar under the angular momentum $\underline{j_1}$ denotes a multiplication factor $(2j_1+1)^{-1/2}$. Also we will use multiple bars to indicate multiple factors. To prove this rule, we simply note that for a null block β, Rule II becomes

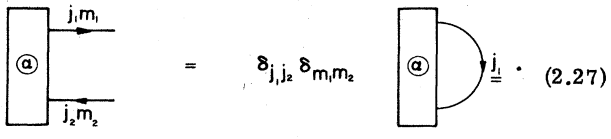

(2.27)

This transformation rule results from the rotational invariance of the corresponding matrix element.

From these two fundamental rules, we can easily derive besides others the following additional useful rules:

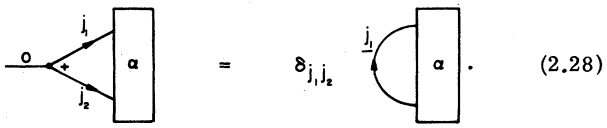

(2.28)

The direction of the linked line j_1 in the right-hand side of (2.28) may be remembered by noting that in the left-hand-side diagram the "+" sign indicates the coupling of j_2 to j_1.

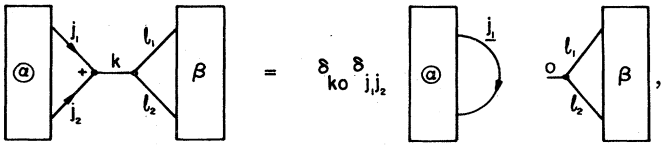

(2.29)

where the direction of the line k is immaterial.

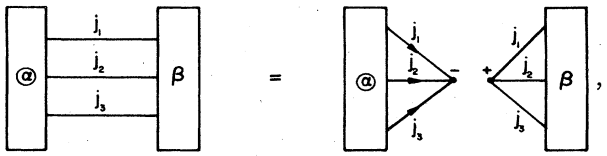

(2.30)

where in the left-hand-side diagram the directions (or variances) of the lines j_1, j_2, and j_3 are arbitrary so long as they stay the same after the factorization.

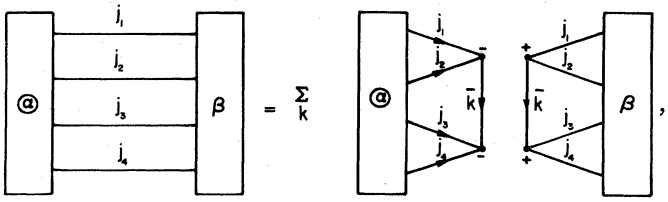

(2.31)

where, as in (2.30), the unspecified directions (or variances) remain the same after the factorization.

The transformation rules I and II and the rules derived from them allow one to join diagrams together or to factor out basic diagrams for which analytical values have been tabulated. Some of those basic diagrams are presented in the next subsection. In applying these transformation rules to a particular diagram in hand, we can change the sign of a node or the direction of a line along with a compensation phase factor. The variances of open angular momentum lines may also be changed by noting the relations (2.13), (2.15), and (2.16); however, transformations of this kind are usually unnecessary. In simplifying phase factors, it is useful to note that $j_1 \pm j_2 \pm j_3$, $j_1 \pm m_1$, etc., are integers if j_1, j_2, and j_3 are components of a 3-jm coefficient.

E. Analytical values of some basic diagrams

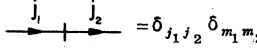

(2.32)

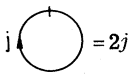

$$= 2j+1 \,, \tag{2.33}$$

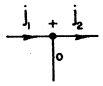

$$= (2j_1+1)^{-1/2}\delta_{j_1 j_2}\delta_{m_1 m_2} \,, \tag{2.34}$$

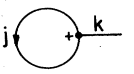

$$= (2j+1)^{1/2}\delta_{k0} \,, \tag{2.35}$$

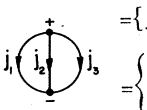

$$= \{j_1\ j_2\ j_3\},\ 3-j \text{ symbol}$$
$$= \begin{cases} 1 & \text{if } |j_1 - j_2| \le j_3 \le (j_1 + j_2), \\ 0 & \text{otherwise}, \end{cases} \tag{2.36}$$

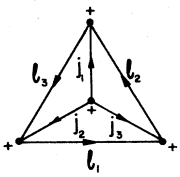

$$= \begin{Bmatrix} j_1 & j_2 & j_3 \\ l_1 & l_2 & l_3 \end{Bmatrix} \,, \quad 6-j \text{ symbol}, \tag{2.37}$$

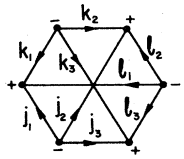

$$= \begin{Bmatrix} j_1 & j_2 & j_3 \\ l_1 & l_2 & l_3 \\ k_1 & k_2 & k_3 \end{Bmatrix} \,, \quad 9-j \text{ symbol} \,. \tag{2.38}$$

In general, we have

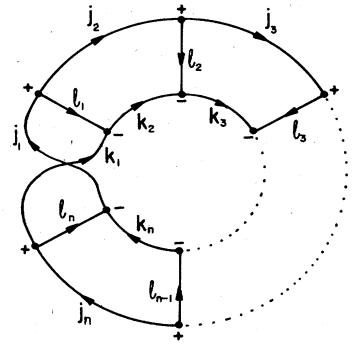

$$= \left\{ \begin{matrix} j_1 & j_2 \cdots j_n \\ l_1 & l_2 \cdots l_n \\ k_1 & k_2 \cdots k_n \end{matrix} \middle| 1 \right\}, \tag{2.39}$$

which is defined as *the 3n-j symbol of the first kind*. For $n=1$, 2, 3, it equals the ordinary $3n$-j symbol within a phase factor. We also have *the 3n-j symbol of the second kind*

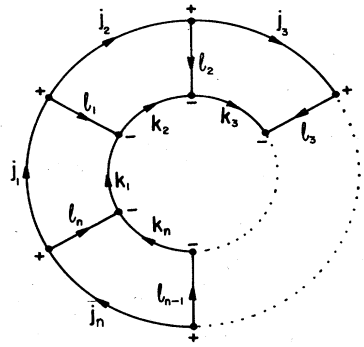

$$= \left\{ \begin{matrix} j_1 & j_2 \cdots j_n \\ l_1 & l_2 \cdots l_n \\ k_1 & k_2 \cdots k_n \end{matrix} \middle| 2 \right\}. \tag{2.40}$$

Further discussion of these $3n$-j symbols may be found in the works by Jucys *et al.* (1962) and by El-Baz and Castel (1972). We emphasize that it is the topology of an angular momentum diagram (i.e., how the various lines in it are connected to each other) which determines its analytical value. Therefore by keeping the topology, we can deform an angular momentum diagram in any way without changing its analytical value.

A very complete tabulation of Clebsch–Gordan coefficients can be found in *Tables of the Clebsch–Gordan Coefficients*, compiled by the Institute of Atomic Energy, Academica Sinica (1965). Extensive tabulation of the Wigner 3-j symbol and the 6-j symbol may be found in the work by Rotenberg *et al.* (1959). This reference also contains extensive references in the literature on $3n$-j symbols.

III. ANALYTICAL EXPANSION OF ANTISYMMETRIZED MATRIX ELEMENTS

The method of evaluating matrix elements between *antisymmetrized many-particle states* is outlined analytically in this section. The part of the manipulation which can be performed more expediently by a graphical procedure is presented again in detail with graphical representation in the next section.

In the Dirac–Fock or Dirac–Fock–Slater description of a many-particle system, a *configuration* is specified by the number of equivalent particles occupying each subshell. In general, there are N_a particles in the subshell j_a, N_b particles in the subshell $j_b, \ldots$, N_λ particles in the subshell j_λ, etc. Accordingly this configuration is denoted by

$$\{j_a^{N_a} j_b^{N_b} \cdots j_\lambda^{N_\lambda} \cdots\}.$$

For reference purpose, we may order the subshells in a certain sequence (e.g., $1s_{1/2}$, $2s_{1/2}$, $2p_{1/2}$, etc., for atomic subshells) and refer them by successive values of the index λ.

We consider states of the many-particle system in which each subshell λ of equivalent particles is in a definite subshell state with the total subshell angular momentum J_λ. Within a subshell λ, if there are several states with the same total subshell angular momentum J_λ, there will be additional quantum numbers α_λ which are required to specify a subshell state uniquely. This coupling scheme is indicated by

$$(j_a^{N_a})\alpha_a J_a (j_b^{N_b})\alpha_b J_b \cdots (j_\lambda^{N_\lambda})\alpha_\lambda J_\lambda \cdots \,.$$

All the total subshell angular momenta $(J_a J_b \cdots J_\lambda \cdots)$ are henceforth coupled successively to form a grand total angular momentum J of the whole many-particle system. After antisymmetrization, such a state is denoted by

$$|[(j_a^{N_a})\alpha_a J_a (j_b^{N_b})\alpha_b J_b \cdots (j_\lambda^{N_\lambda})\alpha_\lambda J_\lambda \cdots] \alpha J M\rangle \,, \tag{3.1}$$

where α stands symbolically for the coupling scheme of total subshell angular momenta.

We will first express the matrix element between *antisymmetrized many-particle states* (3.1) as a sum of matrix elements between *semisymmetrized many-par-*

ticle states. As mentioned in Sec. I, the semisymmetrized many-particle state is defined as the many-particle state which is antisymmetric within each subshell but is not antisymmetric with respect to exchange of two particles from different subshells. Each semisymmetrized matrix element is then expanded in terms of *jm-scheme matrix elements*. After the evaluation of *jm*-scheme matrix elements, we obtain the expansion of the antisymmetrized matrix element in terms of radial integrals.

A. Expansion of antisymmetrized matrix elements in terms of semisymmetrized matrix elements

We consider matrix elements of one-particle operators and two-particle operators in turn.

1. One-particle operator

We define the one-particle operator by

$$V^{(1)}=\sum_{i=1}^{N} v_i \,. \tag{3.2}$$

From the general consideration of de-Shalit and Talmi (1963) and, particularly, of Fano (1965), we can easily deduce the result

$$\begin{aligned}\langle V^{(1)}\rangle \equiv &\Big\langle [(j_a^{N_a})\alpha_a J_a\cdots(j_b^{N_b})\alpha_b J_b\cdots]\,\alpha J M \Big| \sum_{i=1}^{N} v_i \\ &\Big| [(j_a^{N'_a})\alpha'_a J'_a\cdots(j_b^{N'_b})\alpha'_b J'_b\cdots]\,\alpha' J' M'\Big\rangle \\ &=\sum_{ab}\langle V^{(1)}\rangle_{ab}\,,\end{aligned} \tag{3.3}$$

where the summation is over all nonvanishing subshell pairs (a,b) with each pair counted once, and $\langle V^{(1)}\rangle_{ab}$ is defined as

$$\langle V^{(1)}\rangle_{ab}=(-)^{P_{ab}}(N_a N'_b)^{1/2}\langle q(a)\alpha J M|v_N|\,q'(b)\alpha' J' M'\rangle \tag{3.4}$$

with

$$P_{ab}=\sum_{\lambda=a+1}^{b} N_\lambda \,. \tag{3.5}$$

Here $\langle q(a)\alpha J M|$ and $|\,q'(b)\alpha' J' M'\rangle$ are semisymmetrized many-particle states with definite particle distributions specified by $q(a)$ and $q'(b)$, respectively. Explicitly $q(a)$ and $q'(b)$ denote the particle distributions in which the Nth particle (i.e., *the active particle*) is in subshells a and b, respectively, while all the other particles (i.e., *the spectator particles*) assume the same distribution in both states. We emphasize that how the spectator particles are distributed among subshells is immaterial so long as they keep the same distribution in both states.

2. Two-particle operator

We define the two-particle operator by

$$V^{(2)}=\sum_{i<j}^{N} v_{ij} \,. \tag{3.6}$$

Also from the general consideration of de-Shalit and Talmi (1963) and of Fano (1965), we can deduce the result

$$\begin{aligned}\langle V^{(2)}\rangle \equiv &\Big\langle [(j_a^{N_a})\alpha_a J_a\cdots(j_b^{N_b})\alpha_b J_b\cdots(j_c^{N_c})\alpha_c J_c\cdots \\ &\times(j_d^{N_d})\alpha_d J_d\cdots]\,\alpha J M\Big| \\ &\times\sum_{i<j}^{N} v_{ij}\ \Big|[(j_a^{N'_a})\alpha'_a J'_a\cdots(j_b^{N'_b})\alpha'_b J'_b\cdots \\ &\times(j_c^{N'_c})\alpha'_c J'_c\cdots(j_d^{N'_d})\alpha'_d J'_d\cdots]\,\alpha' J' M'\Big\rangle \\ &=\sum_{ab,\,cd}\langle V^{(2)}\rangle_{ab,\,cd}\,,\end{aligned} \tag{3.7}$$

where the summation is over all distinct nonvanishing pairs (ab,cd) with $a\le b$ and $c\le d$, and $\langle V^{(2)}\rangle_{ab,\,cd}$ is defined as

$$\begin{aligned}\langle V^{(2)}\rangle_{ab,\,cd}=&(-)^{P_{abcd}}[N_a(N_b-\delta_{ab})N'_c(N'_d-\delta_{cd})]^{1/2} \\ &\times\{[1+\delta_{ab}\delta_{cd}]^{-1}\langle q(ab)\alpha J M|\,v_{(N-1)N}|\,q'(cd)\alpha' J' M'\rangle \\ &-(1-\delta_{ab})(1-\delta_{cd})\langle q(ab)\alpha J M|v_{(N-1)N}|\,q'(dc)\alpha' J' M'\rangle\}\end{aligned} \tag{3.8}$$

with

$$P_{abcd}=\sum_{\lambda=a+1}^{b}(N_\lambda-\delta_{\lambda b})+\sum_{\lambda=c+1}^{d}(N'_\lambda-\delta_{\lambda d})\,. \tag{3.9}$$

Here $\langle q(ab)\alpha J M|$ denotes a semisymmetrized many-particle state with the $(N-1)$th and Nth particles (the active particles) in subshells a and b, respectively. The states with the distributions $q'(cd)$ and $q'(dc)$ are defined similarly. Again we emphasize that all of them have the same spectator-particle distribution.

B. Expansion of semisymmetrized matrix elements in terms of *jm*-scheme matrix elements

To evaluate matrix elements between semisymmetrized many-particle states we need to single out those particles which actually participate in the interaction, i.e., the active particles [the Nth particle in (3.4) and the $(N-1)$th and Nth particles in (3.8)]. This can be accomplished by fractional parentage expansions of the subshell states involving active particles. With coefficients of fractional parentage (to be referred to as c.f.p.) as expansion coefficients, the semisymmetrized many-particle state can thereby be expressed by a linear combination of parent states. Each of these parent states can then be decoupled into a product of two parts: One contains active particles, and the other contains spectator particles. These expansions and decouplings enable us to express a semisymmetrized matrix element in terms of *jm*-scheme matrix elements. We consider the cases for one-particle operators and for two-particle operators in turn:

1. One-particle operator

To evaluate the semisymmetrized matrix element in (3.4) we first decouple the semisymmetrized many-

particle states as

$$\langle q(a)\alpha JM| = \sum_p C_a(p;\alpha JM)\langle p;q(a)|\langle a| \tag{3.10}$$

and

$$|q'(b)\alpha'J'M'\rangle = \sum_{p'} C_b(p';\alpha'J'M')|p';q'(b)\rangle|b\rangle . \tag{3.11}$$

Here $\langle p;q(a)|$ and $|p';q'(b)\rangle$ denote symbolically the uncoupled subshell states of the spectator particles, i.e., the first $(N-1)$ particles; $\langle a|$ and $|b\rangle$, or explicitly $\langle j_a m_a|$ and $|j_b m_b\rangle$, are the orbitals of the active particle, i.e., the Nth particle. The expansion coefficient $C_a(p;\alpha JM)$ or $C_b(p';\alpha' J' M')$ stands symbolically for the product of a c.f.p. and all the 3-jm coefficients needed in the uncoupling, and the summation index p or p' for the summations over the c.f.p. and magnetic quantum numbers. An explicit example will be given in (4.4) in Sec. IV. B when we consider the graphical procedure. By using (3.10) and (3.11), we can write the semisymmetrized matrix element in (3.4) as

$$\langle q(a)\alpha JM|v_N|q'(b)\alpha'J'M'\rangle = \sum_{pp'} C_a(p;\alpha JM)C_b(p';\alpha'J'M')\langle p;q(a)|p';q'(b)\rangle\langle a|v_N|b\rangle \tag{3.12}$$

Here the matrix element $\langle p;q(a)|p';q'(b)\rangle$ represents a product of overlap integrals and is independent of the interaction. The matrix element $\langle a|v_N|b\rangle$, called *the jm-scheme matrix element*, depends on the interaction and will be evaluated in the next subsection. Readers may refer to (4.15) for the graphical representation of (3.12)

2. Two-particle operator

We decouple the semisymmetrized many-particle states in (3.8) and obtain

$$\langle q(ab)\alpha JM| = \sum_p C_{ab}(p;\alpha JM)\langle p;q(ab)|\langle ab| \tag{3.13}$$

and

$$|q'(cd)\alpha'J'M'\rangle = \sum_{p'} C_{cd}(p';\alpha'J'M')|p';q'(cd)\rangle|cd\rangle . \tag{3.14}$$

Here $\langle p;q(ab)|$ and $\langle p';q'(cd)|$ stand symbolically for the uncoupled subshell states of the spectator particles, i.e., the first $(N-2)$ particles; $\langle ab|$ and $|cd\rangle$, or explicitly $\langle j_a m_a j_b m_b|$ and $|j_c m_c j_d m_d\rangle$, for the states of the active particles, i.e., the $(N-1)$th and Nth particles; $C_{ab}(p;\alpha JM)$ and $C_{cd}(p';\alpha'J'M')$ for the expansion coefficients which are products of c.f.p. and 3-jm coefficients; p and p' for all the summation indices involved. Explicit examples will be given in (4.7) in Sec. IV. B. Note that here a and b (also c and d) may represent either equivalent or nonequivalent orbitals.

By means of the expansions (3.13) and (3.14) we obtain the first semisymmetrized matrix element (the direct term) in (3.8) as

$$\langle q(ab)\alpha JM|v_{N-1,N}|q'(cd)\alpha'J'M'\rangle = \sum_{pp'} C_{ab}(p;\alpha JM)C_{cd}(p';\alpha'J'M')\langle p;q(ab)|p';q'(cd)\rangle \times\langle ab|v_{N-1,N}|cd\rangle . \tag{3.15}$$

Here the matrix element $\langle p;q(ab)|p';q'(cd)\rangle$ represents a product of overlap integrals, and $\langle ab|v_{N-1,N}|cd\rangle$ is a jm-scheme matrix element. The second semisymmetrized matrix element (the exchange term) in (3.8) can be expanded similarly as (3.15) in terms of jm-scheme matrix elements. Readers may refer to (4.16) for the graphical representation of (3.15).

C. *jm*-scheme matrix elements

In the last subsection, we have shown how a semisymmetrized matrix element can be expanded as a sum of products of two parts: One is the interaction-independent part involving the coupling coefficients, and the other is the interaction-dependent part represented by a jm-scheme matrix element. The jm-scheme matrix elements for the cases of one-particle operators and two-particle operators are given by $\langle a|v_N|b\rangle$ and $\langle ab|v_{N-1,N}|cd\rangle$, respectively. For specific operators, these matrix elements can be evaluated analytically in terms of radial integrals. The results for commonly used operators and potentials are presented in Appendix B along with their graphical forms.

In general, any operator can be written as a sum of products of irreducible tensor operators. Hence in this subsection for a general purpose, we consider v_N and $v_{N-1,N}$ to be irreducible tensor operators. The results are given in terms of reduced matrix elements as follows.

1. One-particle operator

Assume the one-particle operator v_N to be an irreducible tensor operator of degree j

$$v_N = T_{jm}(N) . \tag{3.16}$$

By applying the Wigner-Eckart theorem (Wigner, 1927; Eckart, 1930) we obtain the jm-scheme matrix element in (3.12) as

$$\langle a|v_N|b\rangle \equiv \langle j_a m_a|T_{jm}|j_b m_b\rangle = \begin{pmatrix} j_a & m & m_b \\ m_a & j & j_b \end{pmatrix}\langle j_a||T^{(j)}||j_b\rangle . \tag{3.17}$$

Here we denote the angular momentum coupling by a 3-jm coefficient, and $\langle j_a||T^{(j)}||j_b\rangle$ is the reduced matrix element which is usually expressible as a sum of weighted radial integrals for a specific case. It is of interest to note that the bra (covariant) state $\langle j_a m_a|$ corresponds to the covariant component in the 3-jm coefficient, and the contravariant operator T_{jm} and the

ket (contravariant) state $|j_b m_b\rangle$ correspond to the two contravariant components. No extra phase or weight factor, besides the reduced matrix element, is carried by (3.17), and the rotational properties of the matrix element is clearly indicated by the 3-jm coefficient. Furthermore for the covariant tensor operator $T^{\dagger}_{jm}$ [defined in (2.14) as the Hermitian conjugate of T_{jm}], we have

$$\langle j_a m_a | T^{\dagger}_{jm} | j_b m_b \rangle = \begin{pmatrix} j_a & j & m_b \\ m_a & m & j_b \end{pmatrix} \langle j_a \| T^{(j)} \| j_b \rangle . \tag{3.18}$$

To emphasize the fact that the jm-scheme matrix element is separated into a geometric part and a dynamical part, we rewrite (3.17) as

$$\langle a | v_N | b \rangle = G_j(a;b) X_j(a;b) . \tag{3.19}$$

The geometric factor $G_j(a;b)$, which corresponds to a coupling diagram in the graphical representation and will be called *the interaction diagram*, is defined in this simple case as

$$G_j(a;b) = \begin{pmatrix} j_a & m & m_b \\ m_a & j & j_b \end{pmatrix} . \tag{3.20}$$

The interaction strength $X_j(a;b)$ is defined accordingly as

$$X_j(a;b) = \langle j_a \| T^{(j)} \| j_b \rangle . \tag{3.21}$$

Readers may refer to (4.10) for the graphical representation.

2. Two-particle operator

For the case of a two-particle operator, we consider an irreducible tensor of degree j which is the tensorial product of two irreducible tensor operators acting on two different particles, i.e.,

$$v_{N-1,N} = T_{jm}(N-1,N) \equiv \sum_{m_1 m_2} \langle j_1 m_1 j_2 m_2 | jm \rangle T_{j_1 m_1}(N-1) T_{j_2 m_2}(N) . \tag{3.22}$$

As before, by applying the Wigner–Eckart theorem we can obtain the jm-scheme matrix element in (3.15) as

$$\langle ab | v_{N-1,N} | cd \rangle \equiv \langle j_a m_a j_b m_b | T_{jm}(N-1,N) | j_c m_c j_d m_d \rangle = G_{j_1 j_2 j}(ab;cd) X_{j_1 j_2}(ab;cd), \tag{3.23}$$

for which the graphical representation will be given in (4.11). Here the geometric factor $G_{j_1 j_2 j}(ab;cd)$ is given by

$$G_{j_1 j_2 j}(ab;cd) = (2j+1)^{1/2} \sum_{m_1 m_2} \begin{pmatrix} j_a & j_1 & m_c \\ m_a & m_1 & j_c \end{pmatrix} \begin{pmatrix} m_1 & m & j_2 \\ j_1 & j & m_2 \end{pmatrix} \begin{pmatrix} j_b & m & m_2 \\ m_b & j_2 & j_d \end{pmatrix} , \tag{3.24}$$

and the interaction strength by

$$X_{j_1 j_2}(ab;cd) = \langle j_a \| T^{(j_1)} \| j_c \rangle \langle j_b \| T^{(j_2)} \| j_d \rangle . \tag{3.25}$$

D. Expansion of antisymmetrized matrix elements in terms of reduced matrix elements

In Sec. III. A we expanded the matrix element between antisymmetrized many-particle states as a sum of semisymmetrized matrix elements. In Sec. III. B we obtained the semisymmetrized matrix element in terms of jm-scheme matrix elements, which were later evaluated in Sec. III. C. Here we summarize the results.

1. One-particle operator

For $V^{(1)} = \sum_{i=1}^{N} T_{jm}(i)$, the antisymmetrized matrix element (3.3) has been evaluated as

$$\langle \alpha JM | V^{(1)} | \alpha' J' M' \rangle = \sum_{ab} (-)^{P_{ab}} (N_a N'_b)^{1/2} D_{jm}(a;b) X_j(a;b) , \tag{3.26}$$

where the coupling coefficient $D_{jm}(a;b)$ is given by

$$D_{jm}(a;b) = \sum_{pp'} C_a(p;\alpha JM) C_b(p';\alpha' J' M') \langle p; q(a) | p'; q'(b) \rangle G_j(a;b) . \tag{3.27}$$

2. Two-particle operator

For $V^{(2)} = \sum_{i<j}^{N} T_{jm}(ij)$ with $T_{jm}(ij)$ defined in (3.22), we can summarize the results for the antisymmetrized matrix element (3.7) as

$$\langle \alpha JM | V^{(2)} | \alpha' J' M' \rangle = \sum_{ab,\,cd} (-)^{P_{abcd}} [N_a (N_b - \delta_{ab}) N'_c (N'_d - \delta_{cd})]^{1/2} \times \left\{ [1+\delta_{ab}\delta_{cd}]^{-1} D_{jm}(ab;cd) X_{j_1 j_2}(ab;cd) - (1-\delta_{ab})(1-\delta_{cd}) D_{jm}(ab;dc) X_{j_1 j_2}(ab;dc) \right\} \tag{3.28}$$

Here the coupling coefficient $D_{jm}(ab;cd)$ is defined as

$$D_{jm}(ab;cd) = \sum_{pp'} C_{ab}(p;\alpha JM) C_{cd}(p';\alpha' J' M') \langle p; q(ab) | p'; q'(cd) \rangle G_{j_1 j_2 j}(ab;cd) \tag{3.29}$$

with $D_{jm}(ab;dc)$ similarly defined. The interaction strength $X_{j_1 j_2}(ab;cd)$ has been given in (3.25), and $X_{j_1 j_2}(ab;dc)$ is given by a similar expression with c and d interchanged.

IV. GRAPHICAL EVALUATION OF SEMISYMMETRIZED MATRIX ELEMENTS

Evaluation of the coupling coefficients $D_{jm}(a;b)$ and $D_{jm}(ab;cd)$, given in (3.27) and (3.29), respectively, is a formidable task. Although for many cases they may be evaluated numerically (Grant, 1973; 1976) by using a digital computer, these coupling coefficients in general have to be obtained analytically for each particular case, especially for the analytical study of a matrix element. In this section we will show how to obtain an analytical expression of an antisymmetrized many-particle matrix element from easily constructed diagrams.

In Sec. IV.A the graphical procedure of constructing semisymmetrized many-particle states is illustrated by an example. Section IV.B describes how to decouple particles graphically from an antisymmetrized subshell state. *The bra and ket diagram blocks* are also defined there. In Sec. IV.C the jm-scheme matrix element is considered. Its graphical representation is defined as *the interaction block*. Specific diagrams are given for the cases considered analytically in Sec. III.C. Other interaction diagrams for commonly used operators and potentials are presented in Appendix B. In Sec. IV.D *the spectator block* is defined. Evaluation of the joined diagram, called *the recoupling diagram*, is described in Sec. IV.E.

A. Construction of semisymmetrized many-particle states

The construction of diagrams for semisymmetrized many-particle states can easily be carried out in the C–G representation. The procedure is best demonstrated by working with an example.

Consider a configuration having open shells, a, b, c, d, and closed shells λ, etc. A particular coupling scheme of the open shells is represented by

$$|\,[\,(J_a J_b)J_{ab}\,(J_c J_d)J_{cd}\,]JM\rangle$$

where J_a, J_b, J_c, J_d are the total angular momenta of respective subshells, and the parentheses specify the sequence of the couplings. These couplings can be given analytically by

$$\begin{aligned}|\,[\,(J_a J_b)J_{ab}\,(J_c J_d)J_{cd}\,]JM\rangle &= \sum_{M_{ab}M_{cd}} |\,(J_a J_b)J_{ab}M_{ab}\rangle|\,(J_c J_d)J_{cd}M_{cd}\rangle\langle J_{ab}M_{ab}J_{cd}M_{cd}|JM\rangle \\ &= \sum_{M_{ab}M_{cd}} \sum_{M_a M_b} \sum_{M_c M_d} |J_a M_a\rangle|J_b M_b\rangle|J_c M_c\rangle|J_d M_d\rangle \\ &\quad\times\langle J_a M_a J_b M_b|J_{ab}M_{ab}\rangle\langle J_c M_c J_d M_d|J_{cd}M_{cd}\rangle\langle J_{ab}M_{ab}J_{cd}M_{cd}|JM\rangle\,,\end{aligned} \tag{4.1}$$

which corresponds to the graphical representation

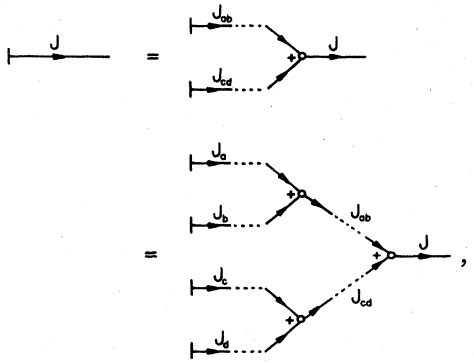

(4.2a)

or simply,

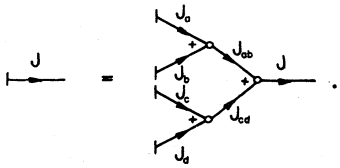

(4.2b)

All the closed shells are represented symbolically by

Hence the semisymmetrized many-particle state has the graphical representation

$$|\,J_\lambda\,[\,(J_a J_b)J_{ab}\,(J_c J_d)J_{cd}\,]JM\rangle$$

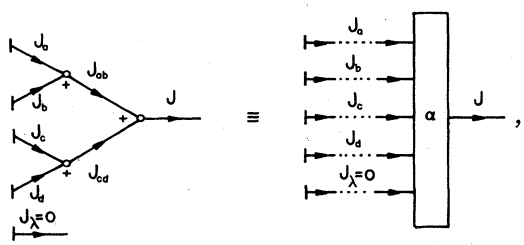

(4.3)

where α denotes the coupling scheme of the open shells.

From the above example we can generalize the following graphical procedure for constructing the semisymmetrized bra or ket states:

(i) Represent the grand total angular momentum by a

line.

(ii) Draw two branches from the grand total angular momentum and a small circle at the vertex. The two angular momentum lines added represent the two angular momenta which are coupled to form the grand total angular momentum. Write a sign, + or −, at the vertex to indicate the order of coupling.

(iii) Repeat step (ii), starting from the new angular momentum lines, until all subshells containing active particles are decoupled.

(iv) Add angular momentum lines for closed shells.

(v) Mark appropriate arrows on the angular momentum lines.

It is more convenient to construct bra (covariant) states from left to right and ket (contravariant) states from right to left. The so-constructed configuration diagrams are to be transformed into diagrams in the 3-jm representation by using the procedure given in Sec. II.C.

B. Decoupling of active particles; bra block and ket block

As states in Sec. III.B, we can single out active particles from a subshell by a fractional parentage expansion. We consider two cases in turn.

1. One-particle coefficient of fractional parentage

To single out one particle from a subshell we use a one-particle fractional parentage expansion, i.e.,

$$\begin{aligned}|(j^n)\alpha JM\rangle &= \sum_{\alpha_1 J_1} [(j^{n-1})\alpha_1 J_1 j\,|\,\alpha J]\\ &\times |(j^{n-1})\alpha_1 J_1 j\, JM\rangle\\ &= \sum_{\substack{\alpha_1 J_1\\ M_1 m}} [(j^{n-1})\alpha_1 J_1 j\,|\,\alpha J]\langle J_1 M_1 jm\,|\,JM\rangle\\ &\times |(j^{n-1})\alpha_1 J_1 M_1\rangle |jM\rangle\ . \end{aligned} \tag{4.4}$$

Here to indicate more clearly the coupling, we use the abbreviated notation

$$[(j^{n-1})\alpha_1 J_1 j\,|\,\alpha J] \equiv [j^{n-1}(\alpha_1 J_1) j J|\}j^n \alpha J] \tag{4.5}$$

for the c.f.p. defined by Racah (1943).

The last expression in (4.4) gives the explicit form of (3.11) in the particular case of one subshell. This decoupling can be represented by the diagram

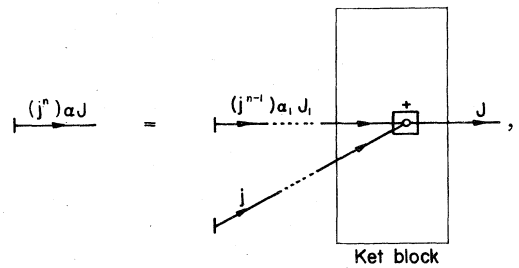

(4.6)

where the c.f.p. $[(j^{n-1})\alpha_1 J_1 j\,|\,\alpha J]$ and the summation over it are implied by the square □ at the vertex $(J_1 j J)$. *The ket block* is defined as the portion of the diagram indicated in (4.6); *a bra block* is similarly defined in the case of a covariant state.

2. Two-particle coefficient of fractional parentage

To single out two particles from a subshell we use a two-particle fractional parentage expansion, i.e.,

$$\begin{aligned}|(j^n)\alpha JM\rangle &= \sum_{\alpha_2 J_2 J'} [(j^{n-2})\alpha_2 J_2 (j^2) J'\,|\,\alpha J]\\ &\times |(j^{n-2})\alpha_2 J_2 (j^2) J' JM\rangle\\ &= \sum_{\substack{\alpha_2 J_2 J'\\ M_2 M'\\ mm'}} [(j^{n-2})\alpha_2 J_2 (j^2) J'\,|\,\alpha J]\\ &\times \langle jmjm'|J'M'\rangle\langle J_2 M_2 J'M'|JM\rangle\\ &\times |(j^{n-2})\alpha_2 J_2 M_2\rangle |jm\rangle |jm'\rangle\ , \end{aligned} \tag{4.7}$$

where we have used the abbreviated notation

$$[(j^{n-2})\alpha_2 J_2 (j^2) J'\,|\,\alpha J] \equiv [j^{n-2}(\alpha_2 J_2) j^2 (J') J|\}j^n \alpha J] \tag{4.8}$$

to represent the two-particle c.f.p. The last expression of (4.7) gives the explicit example for separating two equivalent electrons from a subshell, which was given symbolically in (3.14).

The graphical representation of (4.7) is given by

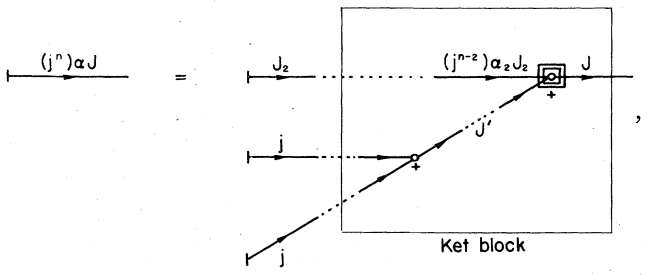

(4.9)

where the two-particle c.f.p. $[(j^{n-2})\alpha_2 J_2 (j^2) J'|\,\alpha J]$ and the summation over it are denoted by the double squares at the vertex $(J_2 J' J)$. The ket block is defined as indicated in (4.9); a bra block is defined in the case of a covariant state.

Tables of c.f.p. may be found in the works of Edmonds and Flowers (1952), de-Shalit and Talmi (1963), and Sivcev *et al.* (1974).

C. Interaction block

An interaction block refers to the diagram block representing $\langle a\,|v_N|\,b\rangle$ in the case of a one-particle operator and $\langle ab\,|v_{N-1,N}|\,cd\rangle$ in the case of a two-particle

operator. These jm-scheme matrix elements have been given analytically for general cases in Sec. III.C. Besides a dynamical multiplication factor, *the interaction strength*, the jm-scheme matrix elements depend only on the rotational properties of the interaction and states involved. We present here the interaction blocks for the general operators worked out in Sec. III.C. Specific examples will be given in Appendix B. Again we consider two cases in turn:

1. One-particle operator

An elementary interaction is represented by an irreducible tensor operator T_{jm} of degree j. Its jm-scheme matrix element was given in (3.19) and has the graphical representation

$\langle a|v_N|b\rangle =$ 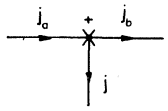

, (4.10)

where the coupling coefficient $G_j(a;b)$ is represented by the coupling diagram, and the interaction strength $X_j(a;b)$ is denoted by the cross "X" at the vertex $(j_a j j_b)$. More complicated interactions can be expressed as a linear combination of this elementary interaction.

2. Two-particle operator

We assume the elementary two-particle interaction to be the irreducible tensor operator $T_{jm}(N-1, N)$ defined in (3.22). Hence from (3.23) we obtain the graphical representation

$\langle ab|v_{N-1,N}|cd\rangle =$ 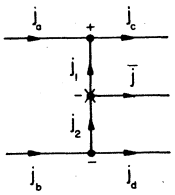

. (4.11)

Here the cross "X" at the vertex $(j_1 j j_2)$ denotes the interaction strength $X_{j_1 j_2}(ab;cd)$; the bar on the angular momentum $\bar{j}$ represents the multiplication factor $(2j+1)^{1/2}$.

D. Spectator block

A spectator block refers to the diagram block representing the scalar product of subshell states or groups of subshell states which do not participate in the interaction considered in the semisymmetrized matrix element. Examples of spectator blocks were given as $\langle p; q(a)|p'; q'(b)\rangle$ in (3.12) and $\langle p; q(ab)|p'; q'(cd)\rangle$ in (3.15). As mentioned in Sec. III.A, the spectator particles have the same distribution among subshells in both the bra and ket states. This fact implies that the scalar product of the composite states can be written as a product of overlap integrals for all subshells. Graphically, we represent spectator blocks as follows.

(i) $\langle p; q(a)|p'; q'(b)\rangle =$ 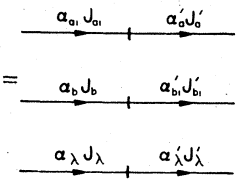

, (4.12)

where $\alpha_{a1}J_{a1}$ and $\alpha'_{b1}J'_{b_1}$ are the states of subshells a and b after the active particle has been decoupled out; $\alpha_\lambda J_\lambda$ and $\alpha'_\lambda J'_\lambda$ denote symbolically all the other subshell states or groups of subshell states. From (2.32) we know that (4.12) represents a product of Kronecker deltas for the states involved, provided we use the same orthonormal set of particle orbitals in both the bra and ket states.

(ii) $\langle p; q(ab)|p'; q'(cd)\rangle =$ 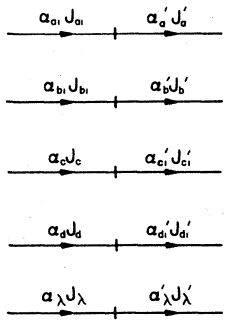

, (4.13)

where the notations are defined similarly as in the case (i). Another example is given by

$\langle p; q(aa)|p'; q'(cd)\rangle$

$=$ 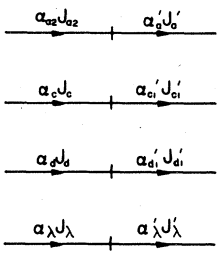

, (4.14)

where $\alpha_{a2}J_{a2}$ is the state of subshell a after two active particles being decoupled out by a two-particle fractional parentage expansion.

The graphical rule implied by (4.12), (4.13), and (4.14) is that we simply join together the corresponding contravariant-covariant angular momentum lines in the bra and ket blocks. Note however that this simple graphical rule does not apply when particle orbitals in the bra state are not orthonormal to those in the ket state. In such cases we need an extra factor which is the product of all the overlap integrals of the spectator particles of the bra and ket states.

E. Evaluation of recoupling diagrams

In Sec. IV.A we demonstrated how to construct diagrams for semisymmetrized many-particle states, and a simple graphical procedure was given. In Sec. IV.B we showed how to graphically separate active particles

from a subshell. There the part of the configuration diagram involving expansion coefficients and angular momentum couplings constituted the bra block or the ket block in the case of a covariant state or contravariant state, respectively. In Sec. IV.C and IV.D, we defined the interaction block and the spectator block; their typical diagrams were given. Here we summarize the results by the symbolic diagrams:

(i) $\langle q(a)\alpha JM \mid v_N \mid q'(b)\alpha' J' M' \rangle$

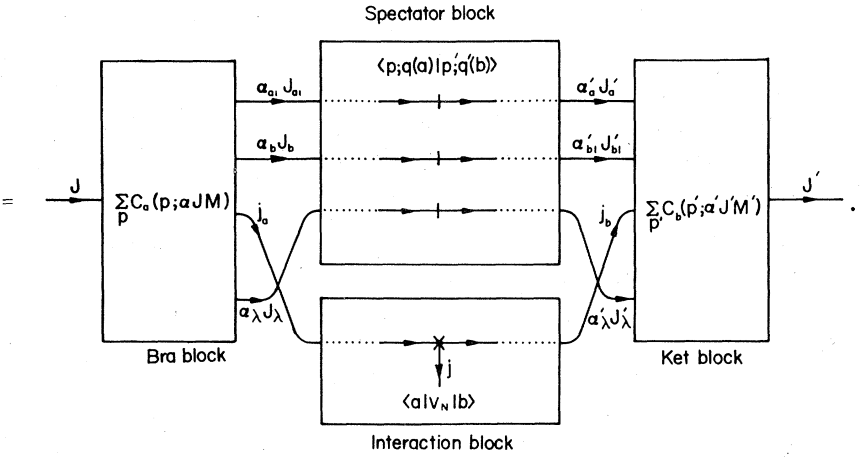

(4.15)

(ii) $\langle q(ab)\alpha JM \mid v_{N-1,N} \mid q'(cd)\alpha' J' M' \rangle$

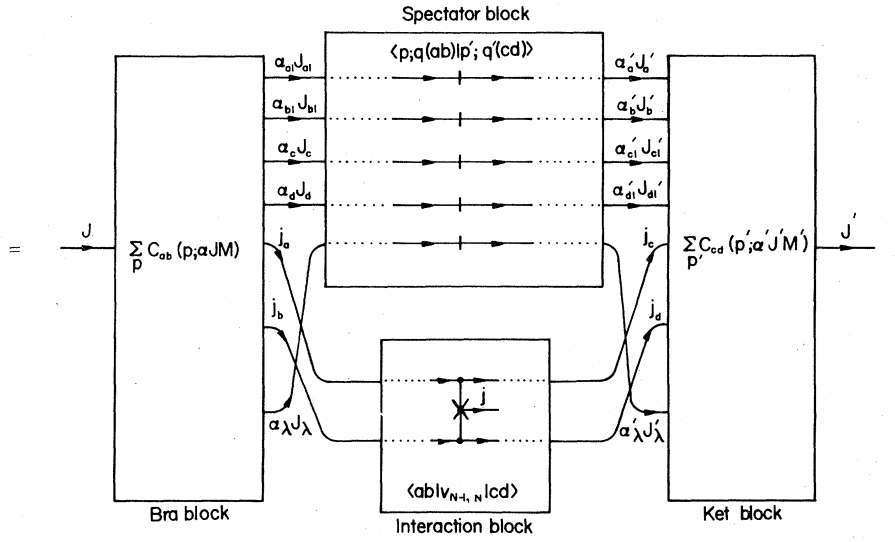

(4.16)

After extracting the interaction strength, c.f.p., and summations over them in (4.15) or (4.16), we are in general left with a pure angular-momentum-coupling diagram, i.e.,

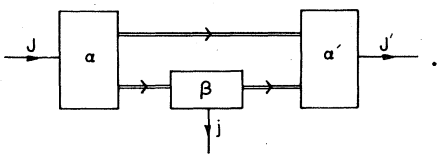

(4.17)

Here the double lines stand symbolically for all angular momentum lines connecting two diagram blocks. By using the transformation rule (2.30), we obtain

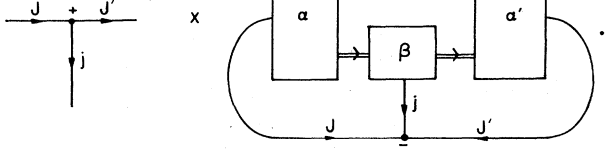

(4.18)

The first factor in (4.18) represents a 3-*jm* coefficient, which is to be expected by applying directly the Wigner-Eckart theorem to the semisymmetrized matrix element. The second factor in (4.18) is a *recoupling diagram* representing analytically a recoupling coefficient. By using transformation rules given in Sec. II.D, we can express the recoupling diagram in terms of products of

$3n$-j diagrams whose analytical values have been tabulated extensively (Rotenberg *et al.*, 1959, Jucys *et al.*, 1962).

The most expedient way to factor graphically a recoupling diagram into $3n$-j diagrams depends, of course, on the particular diagram in question. A simple rule is to look first for diagram blocks separable on one angular momentum line and then on two and three angular momentum lines.

V. SUMMARIZED PROCEDURE FOR EVALUATING ANTISYMMETRIZED MATRIX ELEMENTS

In this section the results of Secs. III and IV will be summarized in the form of a step-by-step procedure by which matrix elements of operators or potentials between antisymmetrized many-particle states can be evaluated. The prescription is given as follows.

(i) Follow (3.3) and (3.4) for one-particle operators or (3.7) and (3.8) for two-particle operators to express the antisymmetrized matrix element as a sum of semisymmetrized matrix elements.

(ii) For each semisymmetrized matrix element, construct graphically semisymmetrized many-particle states:

(a) Begin with the grand total angular momentum and the two angular momenta coupled to it. Here we use the bra state to illustrate the procedure:

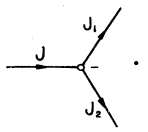

(5.1)

(b) Repeat step (a) starting from J_1 and J_2 until all active subshells are decoupled. Closed shells are then added separately. The resultant diagram is given schematically as

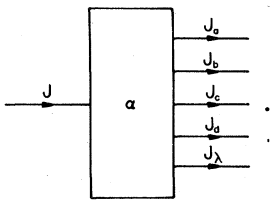

(5.2)

Note that in constructing semisymmetrized many-particle states those subshells which neither contain active particles nor involve coupling with other subshells containing active particles can be ignored.

(c) Decouple active particles from respective subshells by making use of the fractional parentage expansions (4.6) or (4.9), e.g.,

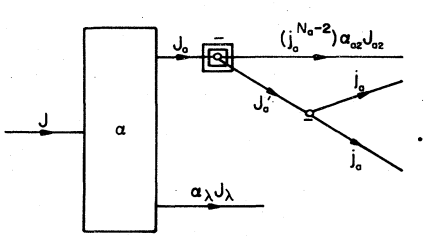

(5.3)

(d) Repeat steps (a), (b), and (c) for the ket state.

(iii) Insert the interaction block between lines representing active particles, and connect the corresponding spectator-particle lines in the bra and ket states. Here the interaction strength in the interaction block can be obtained analytically. A summary of the interaction strengths for various commonly used operators and potentials is given in Appendix B.

(iv) Transform the C–G diagram of the bra and ket states into the 3-jm diagram by using the transformation procedure presented in Sec. II.C.

(v) Transcribe analytical expressions from symbols representing the interaction strength, the c.f.p.'s, and the summations associated with them. The rest of the diagram represents a standard recoupling diagram which may be reduced to an analytical expression. Transformation rules to reduce an arbitrary recoupling diagram to tabulated $3n$-j coefficients is given in Sec. II.D.

(vi) Repeat steps (ii)–(v) for other nonvanishing subshell pairs, as given in step (i). The final expression of the antisymmetrized matrix element is thus obtained by summarizing all the analytical expressions obtained in step (v).

VI. EXAMPLE

We illustrate the graphical procedure by an example: Consider the C–AB; D Auger transition (Auger, 1925; Bambynek *et al.*, 1972) in a rare gas ion, where C denotes the initial vacancy in subshell C, and the final state is characterized by one vacancy in each of subshells A and B plus an outgoing electron D. This is one of the de-excitation processes of an atom with an inner-shell vacancy, in which the transition energy from filling the inner-shell vacancy by an outer-shell electron is carried off by the ejection of another outer-shell electron. The transition probability amplitude is given in the Dirac–Fock formulation by (Huang, 1978a)

$$\boldsymbol{T}_{if}(\mathrm{C-AB;D}) = \langle [J_\lambda (j_a^{n_a})\boldsymbol{\alpha}_a J_a (j_b^{n_b})\boldsymbol{\alpha}_b J_b (j_c^{n_c})\boldsymbol{\alpha}_c J_c]\,\boldsymbol{\alpha} JM| \times \sum_{i<j}^{N} V_{ij} |[J_\lambda (j_a^{n_a'})\boldsymbol{\alpha}_a' J_a' (j_b^{n_b'}) \boldsymbol{\alpha}_b' J_b' (j_c^{n_c'})\boldsymbol{\alpha}_c' J_c' j_d]\,\boldsymbol{\alpha}' J' M'\rangle \tag{6.1}$$

with

$$V_{ij} = \frac{1}{r_{ij}} - (\boldsymbol{\alpha}_i \cdot \boldsymbol{\alpha}_j)\frac{e^{i\omega r_{ij}}}{r_{ij}} + (\boldsymbol{\alpha}_i \cdot \boldsymbol{\nabla}_i)(\alpha_j \cdot \boldsymbol{\nabla}_j)\frac{e^{i\omega r_{ij}} - 1}{\omega^2 r_{ij}}, \tag{6.2}$$

where the bra state is the initial state and the ket state is the final state with j_d the angular momentum of the continuum electron. Here all the other closed shells are denoted symbolically by J_λ. To focus on the essential feature, we assume that the same orthonormal set of single-particle orbitals is used for both the final and initial states. By applying the step-by-step procedure in Sec. V, we evaluate the antisymmetrized matrix element (6.1) as follows.

Step (i): There is only one nonvanishing subshell pair, i.e.,

$$T_{if}(\mathrm{C-AB;D}) = \left\langle \sum_{i<j}^{N} V_{ij} \right\rangle_{ab,cd} \tag{6.3}$$

with

$$\begin{aligned} N_a &= 2j_a+1; \quad N'_a = 2j_a \\ N_b &= 2j_b+1 \quad N'_b = 2j_b \\ N_c &= 2j_c \quad\quad N'_c = 2j_c+1 \\ N_d &= 0 \quad\quad N'_d = 1 \ , \end{aligned} \tag{6.4}$$

and

$$\begin{aligned} P_{abcd} &= \sum_{\lambda=a+1}^{b} (N_\lambda - \delta_{\lambda b}) + \sum_{\lambda=c+1}^{d} (N'_\lambda - \delta_{\lambda d}) \\ &= (\text{even number}) - 1 + (\text{even number}) \\ &= \text{odd number} \ . \end{aligned} \tag{6.5}$$

Here we emphasize that (6.3) is true only when initial and final states are chosen from the same orthonormal set, otherwise more terms appear. From (3.8) we can rewrite (6.3) as

$$\begin{aligned} T_{if}(\mathrm{C-AB;D}) = &-[(2j_a+1)(2j_b+1)(2j_c+1)]^{1/2} \\ &\times \{\langle q(ab)\alpha JM \,|\, V_{N-1,N} | q'(cd)\alpha' J' M' \rangle \\ &- \langle q(ab)\alpha JM \,|\, V_{N-1,N} | q'(dc)\alpha' J' M' \rangle \} \ . \end{aligned} \tag{6.6}$$

The coupling schemes, indicated implicitly by α and α' for the initial and final states, respectively, have not been specified yet. The initial state is composed of closed shells with a vacancy in one of them and therefore has no term structure. The final state consists of two vacancies and one continuum electron. We consider the coupling scheme such that the two almost filled subshells A and B are first coupled to form an ion core specified by the total angular momentum J_{ab}. The core state is then coupled to the continuum orbital D. This coupling scheme of the final state is given explicitly as

$$\langle [(J_a J_b) J_{ab} j_d] JM | \ . \tag{6.7}$$

Now we proceed to evaluate the semisymmetrized matrix elements in (6.6) with the coupling scheme (6.7) for the final state.

A. Direct matrix element

For the first term in the curly brackets in (6.6), we obtain the following.

Step (ii)–(iii): Because those subshells J_λ which neither involve coupling with other subshells nor contain active particles can be ignored, we obtain

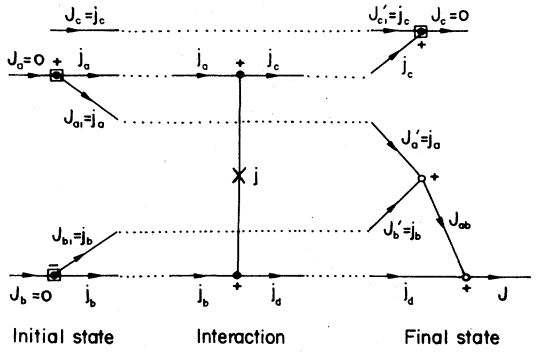

(6.8)

Here the interaction strength, denoted by the cross "X" in the interaction block, of the potential (6.2) can easily be looked up in Appendix B. Note that all the c.f.p. in the diagram (6.8) are trivially unity although we retain the c.f.p. symbols to illustrate the decouplings. Also we have made use of the simple relations (2.20) and (2.21) in decoupling closed shells.

Step (iv): The 3-jm representation of (6.8) is given as

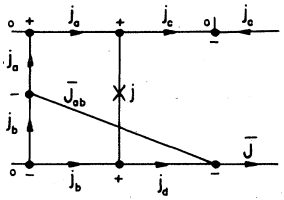

(6.9)

Step (v): We use the transformation rule (2.27) to join the nonzero free angular momentum lines j_c and J,

$\delta_{Jj_c}\delta_{Mm_c}$ 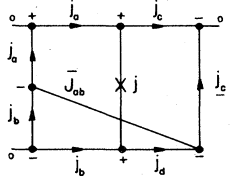

(6.10)

By applying the transformation rule (2.28) to the zero angular momentum lines in (6.10), we obtain the simple diagram

$\delta_{Jj_c}\delta_{Mm_c}$ 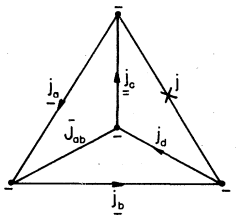

$$= -\delta_{Jj_c}\delta_{Mm_c} \sum_j X_j(ab;cd)(2J_{ab}+1)^{1/2} \times [(2j_a+1)(2j_b+1)(2j_c+1)^2]^{-1/2} \begin{Bmatrix} j_a & j_b & J_{ab} \\ j_d & j_c & j \end{Bmatrix} . \tag{6.11}$$

Here we have used the fact that j_a, j_b, j_c, and j_d are all half-integers to simplify the phase factor.

B. Exchange matrix element

For the second term in the curly brackets in (6.6), we proceed as follows.

Step (ii)–(iii):

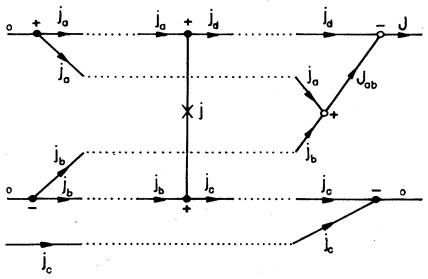

(6.12)

Step (iv):

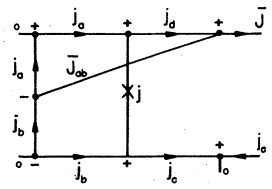

(6.13)

Step (v):

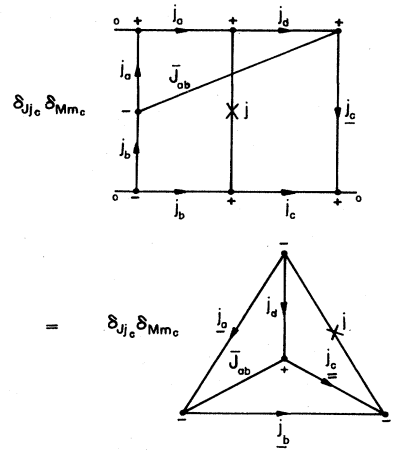

$$= \delta_{Jj_c}\delta_{Mm_c}(-)^{j_c-j_d-J_{ab}}\sum_j X_j(ab;dc)(2J_{ab}+1)^{1/2}$$

$$\times[(2j_a+1)(2j_b+1)(2j_c+1)^2]^{-1/2}\begin{Bmatrix} j_a & j_b & J_{ab} \\ j_c & j_d & j \end{Bmatrix}. \qquad (6.14)$$

C. Antisymmetrized matrix element

Step (vi): By substituting (6.11) and (6.14) into (6.6), we obtain the antisymmetrized matrix element (the transition amplitude) for the C–AB; D Auger transition in a singly ionized closed-shell atom,

$$T_{if}(\text{C–AB; D}) = \delta_{Jj_c}\delta_{Mm_c}\left(\frac{2J_{ab}+1}{2j_c+1}\right)^{1/2}\sum_j\left[X_j(ab;cd)\begin{Bmatrix} j_a & j_b & J_{ab} \\ j_d & j_c & j \end{Bmatrix} + (-)^{j_c-j_d-J_{ab}}X_j(ab;dc)\begin{Bmatrix} j_a & j_b & J_{ab} \\ j_c & j_d & j \end{Bmatrix}\right]. \qquad (6.15)$$

ACKNOWLEDGMENTS

The author would like to acknowledge the hospitality of Professor Bernd Crasemann of the University of Oregon, where this work was begun and was supported in part by the U.S. Army Research Office (Grant DAHCO4-75-G-0021) and by the National Aeronautics and Space Administration (Grant NGR 38-003-036), and of Professor Anthony F. Starace of the University of Nebraska, where the main part of this work was carried out and was supported in part by the U. S. Department of Energy (Contract No. EY-76-S-02-2892. A002). The author would also like to thank Professor Walter R. Johnson and Anthony F. Starace for invaluable comments and suggestions.

APPENDIX A: GLOSSARY OF TERMS

Clebsch-Gordan coefficient, Wigner coefficient

Alternative names for the vector-coupling coefficient.

Wigner 3-j coefficient or symbol

The symmetrized vector-coupling coefficient defined by Wigner (1951).

Covariant 3-jm coefficient or symbol

The vector-coupling coefficient defined in (2.12) in the covariant notation (Wigner, 1959).

3n-j coefficient or symbol

The 3-j symbol is defined as the triangular delta in (2.36). The 6-j and 9-j symbols have their usual meanings while the 12-j symbols and so on are not unique (Edmonds, 1957; Jucys *et al.*, 1962; El-Baz and Castel, 1972).

3n-j coefficients or symbols of the first kind and of the second kind

The symmetrized recoupling coefficients defined by Levinson and Vanagas (1957). Their definitions are given in (2.39) and (2.40), respectively. (Jucys *et al.*, 1962; El-Baz and Castel, 1972).

Subshell

A collection of particle states having the same quantum numbers n, l, and j (or n and κ). (See, e.g., Grant, 1970; Lindgren and Rosen, 1974).

Configuration

A configuration is specified by the number N_λ of equivalent particles occupying each subshell λ and can be denoted by the aggregate $\{N_\lambda\}$.

Antisymmetrized many-particle state

The antisymmetrized state of a configuration. In this work, we mean exclusively the antisymmetrized jj-coupled state in which each subshell of equivalent particles is in a definite total subshell angular momentum state and the whole many-particle system is in a definite grand total angular momentum state.

Antisymmetrized matrix element
The matrix element between antisymmetrized many-particle states.

Semisymmetrized many-particle state
The many-particle state which is antisymmetric within each subshell but is not antisymmetric with respect to exchange of two particles from different subshells.

Semisymmetrized matrix element
The matrix element between semisymmetrized many-particle states.

Active particles
Those particles which actually participate in the interaction in a semisymmetrized matrix element.

Spectator particles
Those particles which, as opposed to active particles, do not participate in the interaction in a semisymmetrized matrix element.

jm-scheme matrix element
The matrix element between uncoupled Dirac single-particle orbitals.

Interaction diagram
The geometric part of the jm-scheme matrix element of an interaction, which depends only on the tensorial properties of the interaction and states involved.

Interaction strength
The dynamical part of the jm-scheme matrix element of an interaction. It can be expressed in terms of reduced matrix elements of tensor operators involved in the interaction.

Interaction block
The diagram block representing the jm-scheme matrix element of an interaction, including the interaction diagram and the interaction strength.

Bra and ket blocks
The diagram blocks representing the angular momentum coupling of the bra and ket states, respectively, of the many-particle system.

Spectator block
The diagram block representing the scalar products of uncoupled spectator-particle states.

Recoupling diagram
The graphical representation of a recoupling coefficient.

APPENDIX B: GRAPHICAL FORMS OF OPERATORS AND POTENTIALS

In this appendix we will consider the jm-scheme matrix elements of one- and two-particle operators, i.e.,

$$\langle a|V|b\rangle \equiv \int d^3r\, U_a^\dagger V U_b \ , \tag{B1}$$

and

$$\langle ab|V_{12}|cd\rangle \equiv \int d^3r_1 \int d^3r_2 U_a^\dagger(1)\, U_a^\dagger(2) V_{12} U_c(1) U_d(2), \tag{B2}$$

and their graphical representations.

Dirac orbitals in a central field can be completely specified by the quantum numbers n, κ, and m. For a definite κ, the total angular momentum quantum number j and the orbital angular momentum quantum number l of the large component, which determines the parity of the Dirac orbital, are given as

$$j = |\kappa| - \frac{1}{2} \ , \quad l = \begin{cases} \kappa & \kappa > 0 \ , \\ -\kappa - 1 & \kappa < 0. \end{cases} \tag{B3}$$

For example, the values $\kappa = -1$, 1, -2, and 2 correspond to $s_{1/2}$, $p_{1/2}$, $p_{3/2}$, and $d_{3/2}$ orbitals, respectively. The magnetic quantum number m is associated with the z component J_z of the total angular momentum. The Dirac orbitals in (B1) and (B2) are assumed to be eigenstates with definite $n\kappa m$ and have the explicit form

$$U_{n\kappa m} = \frac{1}{r} \begin{pmatrix} iG_{n\kappa}(r)\Omega_{\kappa m} \\ F_{n\kappa}(r)\Omega_{-\kappa m} \end{pmatrix} . \tag{B4}$$

Here the radial functions $G_{n\kappa}$ and $F_{n\kappa}$ are the large and small components, respectively, and satisfy the orthonormality condition

$$\int_0^\infty dr (G_{n\kappa} G_{n'\kappa} + F_{n\kappa} F_{n'\kappa}) = \delta_{nn'} \ . \tag{B5}$$

The angular functions $\Omega_{\kappa m}$ in (B4) are normalized spherical spinors defined as

$$\Omega_{\kappa m} \equiv \Omega_{jlm} = \sum_{M\mu} \langle l M \tfrac{1}{2}\mu | jm\rangle\, Y_{lM}(\Omega)\chi_\mu \tag{B6}$$

where Y_{lm} are spherical harmonics, and χ_μ are spin eigenfunctions with $s = 1/2$ and $s_z = \mu$ given, for example, by two-component Pauli spinors. We will evaluate (B1) and (B2) in terms of radial integrals for commonly used operators and potentials.

We first define various functions, notations, and coefficients and present a few useful formulas.

(i) Different combinations of radial wavefunctions

$$\begin{aligned} W_{ab}(r) &= G_a(r)\, G_b(r) + F_a(r) F_b(r) \\ Y_{ab}(r) &= G_a(r) G_b(r) - F_a(r) F_b(r) \\ V_{ab}(r) &= G_a(r) F_b(r) + F_a(r) G_b(r) \\ U_{ab}(r) &= G_a(r) F_b(r) - F_a(r) G_b(r) \\ P_{ab}(r) &= U_{ab}(r) + \frac{(\kappa_b - \kappa_a)}{j} V_{ab}(r) \\ Q_{ab}(r) &= -U_{ab}(r) + \frac{(\kappa_b - \kappa_a)}{j+1} V_{ab}(r) \end{aligned} \tag{B7}$$

(ii) Various radial functions:

$$R_l(r_1 r_2) = r_<^{\,l}/r_>^{\,l+1} \ , \tag{B8}$$

where $r_<$ ($r_>$) is the smaller (larger) of r_1 and r_2.

$$g_l(r_1 r_2) = i\omega j_l(\omega r_<) h_l(\omega r_>) \ , \tag{B9}$$

where j_l and h_l are the spherical Bessel and Hankel functions, respectively.

$$v_l(12) = \epsilon(r_1 - r_2)[R_{l+1}(r_1 r_2) - R_{l-1}(r_1 r_2)] \tag{B10}$$

with $\epsilon(r_1 - r_2)$ the Heaviside step function

$$\epsilon(x) = \begin{cases} 1 & x \geq 0 \ , \\ 0 & x < 0 \ . \end{cases}$$

$$s_l(r_1 r_2) = \begin{cases} -\dfrac{i}{r_1} j_{l+1}(\omega r_2) h_l(\omega r_1), & r_1 > r_2 \ , \\ \dfrac{r_1^{\,l-1}}{\omega^2 r_2^{\,l+2}} - \dfrac{i}{r_1} j_l(\omega r_1) h_{l+1}(\omega r_2), & r_1 < r_2 \ . \end{cases} \tag{B11}$$

$$t_l(r_1 r_2) = \begin{cases} \dfrac{r_2^{\,l-1}}{\omega^2 r_1^{\,l+2}} - \dfrac{i}{r_1} j_{l-1}(\omega r_2) h_l(\omega r_1), & r_1 > r_2 \ , \\ -\dfrac{i}{r_1} j_l(\omega r_1) h_{l-1}(\omega r_2), & r_1 < r_2 \ . \end{cases} \tag{B12}$$

(iii) The following notations are used to denote integrals:

$$\langle f(\boldsymbol{r}) \rangle = \int_0^\infty dr f(r) \ , \tag{B13}$$

$$\langle P_{ab}(r_2) R_j(r_1 r_2) \rangle_2^{\text{even}} = \pi(l_a j l_b) \int_0^\infty dr_2 P_{ab}(r_2) R_j(r_1 r_2) \ ,$$

$$\langle P_{ac}(r_1) R_j(r_1 r_2) Q_{bd}(r_2) \rangle^{\text{even}} \tag{B14}$$

$$= \pi(l_a j l_c)\pi(l_b j l_d) \times \int_0^\infty dr_1 \int_0^\infty dr_2 P_{ac}(r_1) R_j(r_1 r_2) Q_{bd}(r_2) \ , \tag{B15}$$

$$\langle P_{ac}(r_1) R_j(r_1 r_2) Q_{bd}(r_2) \rangle^{\text{odd}}$$

$$= \pi(l_a j+1 l_c)\pi(l_b j+1 l_d) \times \int_0^\infty dr_1 \int_0^\infty dr_2 P_{ac}(r_1) R_j(r_1 r_2) Q_{bd}(r_2), \tag{B16}$$

where the parity selection function is defined as

$$\pi(l_a j l_b) = \begin{cases} 1 & \text{for } l_a + j + l_b \text{ even}, \\ 0 & \text{for } l_a + j + l_b \text{ odd} \ . \end{cases} \tag{B17}$$

(iv) Define the coefficients

$$C_j(a;b) = (-)^{j_a + 1/2}[(2j_a+1)(2j_b+1)]^{1/2} \begin{pmatrix} j_a & j & j_b \\ \frac{1}{2} & 0 & -\frac{1}{2} \end{pmatrix} , \tag{B18}$$

$$C_j(ab;cd) = (-)^{j_1 + j_d}[(2j_a+1)(2j_b+1)(2j_c+1)(2j_d+1)]^{1/2} \times \begin{pmatrix} j_a & j & j_c \\ \frac{1}{2} & 0 & -\frac{1}{2} \end{pmatrix} \begin{pmatrix} j_b & j & j_d \\ \frac{1}{2} & 0 & -\frac{1}{2} \end{pmatrix} , \tag{B19}$$

$$C_{jm}(a;b) = \left(\frac{2j+1}{4\pi}\right)^{1/2} C_j(a;b) \begin{pmatrix} j_a & m & m_b \\ m_a & j & j_b \end{pmatrix} \ . \tag{B20}$$

$$I_j(\kappa_a m_a, \ \kappa_b m_b) = \int d\Omega^\dagger_{\kappa_b m_a} Y_{jm} \Omega_{\kappa_a m_b} = \pi(l_a j l_b) C_{jm}(a;b) \ . \tag{B21}$$

(v) The vector-spherical-harmonics expansion of $U_a^\dagger \boldsymbol{\alpha} U_b$:

$$U_a^\dagger \boldsymbol{\alpha} U_b = \frac{i}{r^2} \sum_{jlm} C_{jm}(a;b) \phi_{jl}(r) \mathbf{Y}^\dagger_{jlm}(\hat{r}) \ , \tag{B22}$$

$$\phi_{j(j-1)} = \pi(l_a j l_b)[j/(2j+1)]^{1/2} P_{ab}(r) \ ,$$

$$\phi_{jj} = \pi(l_a j+1 l_b)[j(j+1)]^{-1/2}(\kappa_a + \kappa_b) V_{ab}(r) \ ,$$

$$\phi_{j(j+1)} = \pi(l_a j l_b)[(j+1)/(2j+1)]^{1/2} Q_{ab}(r) \ . \tag{B23}$$

This was first derived by Mann and Johnson (1971), and we have verified it independently. Since no derivation has previously been given for this extremely useful formula, we present its derivation in Appendix C. Many of the techniques of the vector-spherical-harmonics expansion may be found in various books (Rose, 1957 ; Edmunds, 1957; Akhiezer and Berestetskii, 1965).

(vi) The vector-spherical-harmonics expansion of B(1),

$$\mathrm{B}(1) = \boldsymbol{\nabla}_1 \int d^3 r_2 [U_b^\dagger(2) \boldsymbol{\alpha}_2 U_d(2)] \circ \boldsymbol{\nabla}_2 [(e^{i\omega r_{12}} - 1)/(\omega^2 r_{12})] , \tag{B24}$$

is given as (Huang, 1978a)

$$\mathrm{B}(1) = i \sum_{jlm} C_{jm}(d;b) \psi_{jl}(r_1) \mathbf{Y}_{jlm}(\hat{r}_1) \ , \tag{B25}$$

where

$$\psi_{j(j-1)} = [j/(2j+1)^3]^{1/2} \langle j g_{j-1} P_{bd}(r_2) - (j+1)[g_{j+1} + (2j+1)s_j] Q_{bd}(r_2) \rangle_2^{\text{even}} \ ,$$

$$\psi_{jj} = 0 \ ,$$

$$\psi_{j(j+1)} = [(j+1)/(2j+1)^3]^{1/2} \langle (j+1) g_{j+1} Q_{bd}(r_2) - j[g_{j-1} + (2j+1)t_j] P_{bd}(r_2) \rangle_2^{\text{even}} . \tag{B26}$$

In the limit $\omega \to 0$, we have

$$\mathrm{B}(1) = -\frac{1}{2} \boldsymbol{\nabla}_1 \int d^3 r_2 \, U_b^\dagger(2) \boldsymbol{\alpha} U_d(2) \cdot \boldsymbol{\nabla}_2 r_{12} \ , \tag{B27}$$

and the radial function ψ_{jl} in (B26) becomes

$$\psi_{j(j-1)} = j^{1/2} \left\langle \frac{j}{2j-1} R_{j-1} P_{bd}(r_2) - \frac{j+1}{2} v_j(21) Q_{bd}(r_2) \right\rangle_2^{\text{even}} ,$$

$\psi_{jj}=0$,

$$\psi_{j(j+1)}=(j+1)^{1/2}\left\langle\frac{j+1}{2j+3}R_{j+1}Q_{bd}(r_2)-\frac{j}{2}v_j(12)P_{bd}(r_2)\right\rangle_2^{\text{even}}. \tag{B28}$$

1. One-particle operator

We will present the jm-scheme matrix elements of the operator $f(r)$, β, $\boldsymbol{\alpha}\cdot\mathbf{p}$, $\boldsymbol{\alpha}$, $\mathbf{r}$, and $\boldsymbol{\alpha}\,e^{i\mathbf{k}\cdot\mathbf{r}}$ in turn.

(i) $\langle a|f(r)|b\rangle=\delta_{\kappa_a\kappa_b}\delta_{m_am_b}\langle W_{ab}f(r)\rangle$

$$=\quad \overset{j_a}{\longrightarrow}\!\times\!\overset{j_b}{\longrightarrow}\ , \tag{B29}$$

where the interaction strength, denoted by the cross "X" in (B29), is

$$X(a;b)=\delta_{l_al_b}\langle W_{ab}f(r)\rangle\,. \tag{B30}$$

Note that $\delta_{\kappa_a\kappa_b}\equiv\delta_{j_aj_b}\delta_{l_al_b}$.

(ii) $\langle a|\beta|b\rangle=$ 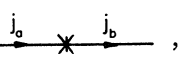 , (B31)

where

$$X(a;b)=\delta_{l_al_b}\langle Y_{ab}\rangle\,. \tag{B32}$$

(iii) The matrix element of $\boldsymbol{\alpha}\cdot\mathbf{p}$ may be obtained by making use of the formula

$$\langle a|\boldsymbol{\alpha}\cdot\mathbf{p}|b\rangle=-i\langle a|\boldsymbol{\alpha}\cdot\hat{r}|b'\rangle \tag{B33}$$

with the understanding that $|b'\rangle$ denotes the Dirac orbital with the substitutions

$$\begin{aligned}G_b(r)\to G_{b'}(r)&=\left(\frac{d}{dr}+\frac{\kappa_b}{r}\right)G_b(r)\,,\\ F_b(r)\to F_{b'}(r)&=\left(\frac{d}{dr}-\frac{\kappa_b}{r}\right)F_b(r)\,,\end{aligned} \tag{B34}$$

for the radial parts of the orbital $|b\rangle$. By using the expansion (B22) and the formula

$$\int d\Omega\,\hat{r}\cdot\mathbf{Y}_{jlm}=-\sqrt{4\pi}\ \delta_{j0}\delta_{l1}\delta_{m0}\,, \tag{B35}$$

we can easily obtain the result

$$G_{jl}(a;b)=(2j+1)^{1/2}\begin{pmatrix}j_a & j & m_b\\ m_a & m_b-m_a & j_b\end{pmatrix}\begin{pmatrix}m_b-m_a & l & 1\\ j & m_b-m_a-q & q\end{pmatrix}$$

$$=$$ 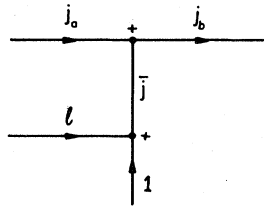 , (B46)

and the interaction strength is

$$X_{jl}(a;b)=\hat{e}_qC_j(a;b)(4\pi)^{1/2}\,i^{1-l}\,Y_{l(m_b-m_a-q)}(\hat{k})D_{jl} \tag{B47}$$

with D_{jl} given as

$$D_{jl}=\begin{cases}-(j)^{1/2}\langle P_{ab}j_{j-1}\rangle^{\text{even}}, & l=j-1,\\ (j)^{-1/2}(\kappa_a+\kappa_b)\langle V_{ab}j_j\rangle^{\text{odd}}, & l=j,\\ -(j+1)^{1/2}\langle Q_{ab}j_{j+1}\rangle^{\text{even}}, & l=j+1.\end{cases}$$

$$\langle a|\boldsymbol{\alpha}\cdot\mathbf{p}|b\rangle=\delta_{\kappa_a\kappa_b}\delta_{m_am_b}\langle U_{ab'}\rangle\,. \tag{B36}$$

This agrees with the result obtained using other methods (see, e.g., Rose, 1957; Grant, 1970). Hence the graphical representation is

$\langle a|\boldsymbol{\alpha}\cdot\mathbf{p}|b\rangle=$ 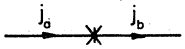 (B37)

with the interaction strength

$$X(a;b)=\delta_{l_al_b}\langle U_{ab'}\rangle\,. \tag{B38}$$

(iv) By using the expansion (B22) and the formula (B21), we obtain

$$\langle a|\boldsymbol{\alpha}|b\rangle=\begin{pmatrix}j_a & 1 & m_b\\ m_a & m_b-m_a & j_b\end{pmatrix}C_1(a;b)I_1(a;b)\,, \tag{B39}$$

where the radial integral is

$$I_1(a;b)=i\hat{e}_{\ -m_a}\langle P_{ab}\rangle^{\text{even}}\,. \tag{B40}$$

Here $\hat{e}_q$ is the spherical unit vector (Edmonds, 1957). Therefore its graphical representation is

$\langle a|\boldsymbol{\alpha}|b\rangle=$ 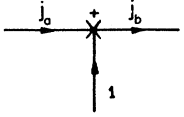 (B41)

with the interaction strength

$$X_1(a;b)=C_1(a;b)I_1(a;b)\,. \tag{B42}$$

(v) For $\langle a|\mathbf{r}|b\rangle$ we obtain the same interaction diagram as (B41) with the radial integral given by

$$I_1(a;b)=-\hat{e}_{m_b-m_a}\langle W_{ab}r\rangle^{\text{even}}\,. \tag{B43}$$

(vi) For $\langle a|\boldsymbol{\alpha}\,e^{i\mathbf{k}\cdot\mathbf{r}}|b\rangle$ we use the expansion (B22) and the familiar Rayleigh expansion of a plane wave,

$$e^{i\mathbf{k}\cdot\mathbf{r}}=4\pi\sum_{l=0}i^lj_l(kr)\sum_{m=-l}^{l}Y^*_{lm}(\hat{r})\,Y_{lm}(\hat{k})\,. \tag{B44}$$

The rest of the calculation is straightforward, and the result is

$$\langle a|\boldsymbol{\alpha}\,e^{i\mathbf{k}\cdot\mathbf{r}}|b\rangle=\sum_{\substack{jl\\ q}}G_{jl}(a;b)X_{jl}(a;b)\,. \tag{B45}$$

Here the interaction diagram is

2. Two-particle operator

We will deal only with rotational invariant interactions, which are generally linear combinations of zero-rank tensors obtained by contracting tensors of the same rank. The matrix element of these interactions can be calculated with the result (Huang, 1977, 1978a, and 1978b)

$$\langle ab\,|\,V(r_{12})\,|\,cd\rangle = \sum_j G_j(ab;cd)\,X_j(ab;cd)\,, \tag{B49}$$

where the interaction diagram is

$$G_j(ab;cd) = \begin{pmatrix} j_a & j & m_c \\ m_a & m_c-m_a & j_c \end{pmatrix} \begin{pmatrix} j_b & m_d & m_c-m_a \\ m_b & j_d & j \end{pmatrix}$$

$$= \tag{B50}$$

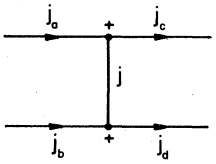

and the interaction strength is

$$X_j(ab;cd) = C_j(ab;cd)\,I_j(ab;cd)\,. \tag{B51}$$

Here $I_j(ab;cd)$ is defined in terms of radial integrals, depending on the specific form of $V(r_{12})$. We summarize the results for various potentials:

(i) *Coulomb potential*: $1/r_{12}$

$$I_j(ab;cd) = \langle W_{ac} R_j W_{bd}\rangle^{\text{even}}\,. \tag{B52}$$

(ii) *Covariant photon interaction*: $(1-\boldsymbol{\alpha}_1\cdot\boldsymbol{\alpha}_2)(e^{i\omega r_{12}}/r_{12})$

$$I_j(ab;cd) = (2j+1)\,\langle W_{ac} g_j W_{bd}\rangle^{\text{even}} - (1-\delta_{j0})(\kappa_a+\kappa_c)(\kappa_b+\kappa_d)\,\frac{2j+1}{j(j+1)}\,\langle V_{ac} g_j V_{bd}\rangle^{\text{odd}} + j\langle P_{ac} g_{j-1} P_{bd}\rangle^{\text{even}} + (j+1)\,\langle Q_{ac} g_{j+1} Q_{bd}\rangle^{\text{even}}\,. \tag{B53}$$

This is obtained by using the expansion (B22) and the formula

$$\int d\Omega_1\, d\Omega_2 \sum_{\nu=-\lambda}^{\lambda} Y^*_{\lambda\nu}(\hat{r}_1)\, Y_{\lambda\nu}(\hat{r}_2)\, \mathbf{Y}_{jlm}(\hat{r}_1)\circ\mathbf{Y}_{j'l'm'}(\hat{r}_2) = (-)^{j+l+m+1}\,\delta_{jj'}\,\delta_{ll'}\,\delta_{m(-m')}\,\delta_{l\lambda}\,. \tag{B54}$$

(iii) *Transverse photon interaction*:

$$-(\boldsymbol{\alpha}_1\cdot\boldsymbol{\alpha}_2)\,\frac{e^{i\omega r_{12}}}{r_{12}} + (\boldsymbol{\alpha}_1\cdot\boldsymbol{\nabla}_1)(\boldsymbol{\alpha}_2\circ\boldsymbol{\nabla}_2)\left[\frac{e^{i\omega r_{12}}-1}{\omega^2 r_{12}}\right].$$

$$I_j(ab;cd) = -(1-\delta_{j0})(\kappa_a+\kappa_c)(\kappa_b+\kappa_d)\,\frac{2j+1}{j(j+1)}\,\langle V_{ac} g_j V_{bd}\rangle^{\text{odd}} + (\kappa_c-\kappa_a)[\langle V_{ac} g_{j-1} P_{bd}\rangle^{\text{even}} + \langle V_{ac} g_{j+1} Q_{bd}\rangle^{\text{even}}] + j(j+1)[\langle P_{ac}\, s_j\, Q_{bd}\rangle^{\text{even}} + \langle Q_{ac}\, t_j\, P_{bd}\rangle^{\text{even}}]\,. \tag{B55}$$

This is obtained by making use of the expansions (B22) and (B25) and the orthogonality relation

$$\int d\Omega_1\, \mathbf{Y}^\dagger_{jlm}(\hat{r}_1)\cdot\mathbf{Y}_{j'l'm'}(\hat{r}_1) = \delta_{jj'}\,\delta_{ll'}\,\delta_{mm'}\,. \tag{B56}$$

(iv) *Breit interaction*:

$$-\frac{1}{2r_{12}}\left[(\boldsymbol{\alpha}_1\cdot\boldsymbol{\alpha}_2) + \frac{(\boldsymbol{\alpha}_1\cdot\mathbf{r}_{12})(\boldsymbol{\alpha}_2\cdot\mathbf{r}_{12})}{r_{12}^2}\right],$$

which represents the transverse photon interaction in the limit $\omega\to 0$.

$$I_j(ab;cd) = -(1-\delta_{j0})(\kappa_a+\kappa_c)(\kappa_b+\kappa_d)\,\frac{1}{j(j+1)}\,\langle V_{ac} R_j V_{bd}\rangle^{\text{odd}} + \frac{j(j+1)}{2j+1}\left[\frac{1}{2j-1}\,\langle P_{ac} R_{j-1} P_{bd}\rangle^{\text{even}} + \frac{1}{2j+3}\,\langle Q_{ac} R_{j+1} Q_{bd}\rangle^{\text{even}} + \frac{1}{2}\,\langle Q_{ac}\, v_j(12)\, P_{bd}\rangle^{\text{even}} + \frac{1}{2}\,\langle P_{ac}\, v_j(21)\, Q_{bd}\rangle^{\text{even}}\right]. \tag{B57}$$

(v) *Operator $\boldsymbol{\alpha}_1\cdot\boldsymbol{\alpha}_2$, which is proportional to the leading imaginary part (Huang, 1978a) of the transverse photon interaction.*

$$I_j(ab;cd) = -\delta_{j1}\,\langle P_{ac}\rangle^{\text{even}}\,\langle P_{bd}\rangle^{\text{even}}\,. \tag{B58}$$

APPENDIX C: VECTOR-SPHERICAL-HARMONICS OF $U_a^\dagger\,\boldsymbol{\alpha}\,U_b$

From the properties of the normalized spherical spinor $\Omega_{\kappa m}$, we can easily prove that

$$\begin{aligned} &\boldsymbol{\sigma}\cdot\hat{r}\,\Omega_{\kappa m} = -\Omega_{-\kappa m}\,,\\ &\boldsymbol{\sigma}\cdot\mathbf{L}\,\Omega_{\kappa m} = -(\kappa+1)\,\Omega_{\kappa m}\,,\\ &\boldsymbol{\sigma}\cdot i(\hat{r}\times\mathbf{L})\,\Omega_{\kappa m} = (\kappa+1)\,\Omega_{-\kappa m}\,. \end{aligned} \tag{C1}$$

Hence three useful formulas may be derived, i.e.,

$$\begin{aligned} &\int d\Omega\,\Omega^\dagger_{\kappa_a m_a}\,\boldsymbol{\sigma}\,\Omega_{-\kappa_b m_b}\cdot\hat{r}\,Y_{jm} = -I_j(\kappa_a m_a, \kappa_b m_b)\,,\\ &\int d\Omega\,\Omega^\dagger_{\kappa_a m_a}\,\boldsymbol{\sigma}\,\Omega_{-\kappa_b m_b}\circ\mathbf{L}\,Y_{jm} = -(\kappa_a+\kappa_b)\,I_j(-\kappa_a m_a, \kappa_b m_b)\,,\\ &\int d\Omega\,\Omega^\dagger_{\kappa_a m_a}\,\boldsymbol{\sigma}\,\Omega_{-\kappa_b m_b}\circ i(\hat{r}\times\mathbf{L})\,Y_{jm} = (\kappa_b-\kappa_a)\,I_j(\kappa_a m_a, \kappa_b m_b)\,. \end{aligned} \tag{C2}$$

where $I_j(\kappa_b m_b, \kappa_a m_a)$, etc., are defined in (B21). To obtain the vector-spherical-harmonics expansion of $U_a^\dagger\,\boldsymbol{\alpha}\,U_b$, i.e.,

$$U_a^\dagger\,\boldsymbol{\alpha}\,U_b = \sum_{jlm} C_{jlm}(r)\,\mathbf{Y}_{jlm}(\hat{r})\,, \tag{C3}$$

we simply evaluate the expansion coefficient as

$$C_{jlm}(r) = \int d\Omega\,\mathbf{Y}^\dagger_{jlm}(\hat{r})\cdot U_a^\dagger\,\boldsymbol{\alpha}\,U_b\,. \tag{C4}$$

By using the formulas (C2) and noting the relations

$$\begin{aligned} &\mathbf{Y}_{j(j-1)m} = (2j+1)^{-1/2}[j^{1/2}\hat{r} - (j+1)^{1/2} i(\hat{r}\times\mathbf{L})]\,Y_{jm}\,,\\ &\mathbf{Y}_{jjm} = [j(j+1)]^{-1/2}\,\mathbf{L}\,Y_{jm}\,,\\ &\mathbf{Y}_{j(j+1)m} = (2j+1)^{-1/2}[-(j+1)^{1/2}\hat{r} - j^{1/2} i(\hat{r}\times\mathbf{L})]\,Y_{jm}\,, \end{aligned}$$

and

$$\boldsymbol{\alpha} = \begin{pmatrix} 0 & \boldsymbol{\sigma} \\ \boldsymbol{\sigma} & 0 \end{pmatrix},$$

we can perform the angular integration of (C4). The expansion (B22) of $U_a^\dagger\,\boldsymbol{\alpha}\,U_b$ is thus obtained.

REFERENCES

Akhiezer, A. I., and V. B. Berestetskii, 1965, *Quantum Electrodynamics* (Wiley, New York).

Auger, P., 1925, J. Phys. Radium 6, 205.

Bambynek, W., B. Crasemann, R. W. Fink, H.-U. Freund, H. Mark, C. D. Swift, R. E. Price, and P. V. Rao, 1972, Rev. Mod. Phys. **44**, 716.

Bolotin, A., Y. Levinson, and V. Tolmacher, 1964, Liet. Fiz. Rinkings **1**, 33.

Bordarier, Y., 1970, thesis, University of Paris.

Briggs, J. S., 1971, Rev. Mod. Phys. **43**, 189.

Brink, D. M., and G. R. Satchler, 1968, *Angular Momentum* (Oxford University, Oxford), Chapter VII.

Condon, E. U., and G. H. Shortley, 1935, *Theory of Atomic Spectra* (Cambridge University, Cambridge).

Danos, M., 1971, Ann. Phys. (N.Y.) **63**, 319.

de-Shalit, A., and I. Talmi, 1963, *Nuclear Shell Theory* (Academic, New York), pp. 263–267.

Dirac, P. A. M., 1930, *The Principle of Quantum Mechanics* (Clarendon, Oxford).

Eckart, C., 1930, Rev. Mod. Phys. **2**, 305.

Edmonds, A. R., 1957, *Angular Momentum in Quantum Mechanics* (Princeton University, Princeton).

Edmonds, A. R., and B. H. Flowers, 1952, Proc. R. Soc. Lond. A **214**, 515.

El-Baz, E., 1969, *Traitement Graphique de L'Algebre des Moments Angulaires* (Masson, Paris).

El-Baz, E., and B. Castel, 1971, Am. J. Phys. **39**, 868.

El-Baz, E., and B. Castel, 1972, *Graphical Methods of Spin Algebras in Atomic, Nuclear, and Particle Physics* (Marcel Dekker, New York).

El-Baz, E., and S. Nahabetian, 1969, Nuovo Cimento Lett. **1**, 583.

Fano, U., 1965, Phys. Rev. **140**, A 67.

Fano, U., and G. Racah, 1959, *Irreducible Tensorial Sets* (Academic, New York).

Grant, I. P., 1970, Adv. Phys. **19**, 747.

Grant, I. P., 1973, Comp. Phys. Commun. **5**, 263.

Grant, I. P., 1976, Comp. Phys. Commun. **11**, 397.

Harter, W. G., and C. W. Patterson, 1976, *A Unitary Calculus for Electronic Orbitals* (Springer, Berlin).

Huang, K.-N., 1977, Phys. Lett. A **63**, 262.

Huang, K.-N., 1978a, J. Phys. B **11**, 787.

Huang, K.-N., 1978b, Phys. Rev. A **18**, 1119.

Huang, K.-N., and A. F. Starace, 1978, Phys. Rev. A **18**, 354.

The Institute of Atomic Energy, Academica Sinica, 1965, *Tables of the Clebsch-Gordan Coefficients* (Science Press, Peking).

Jucys, A. P., and A. A. Bandzaitis, 1967, *Theory of Angular Momentum in Quantum Mechanics* [in Russian] (Mintis, Vilnius).

Jucys, A. P., I. B. Levinson, and V. V. Vanagas, 1962, *The Theory of Angular Momentum* (Israel Program for Scientific Translation, Jerusalem).

Judd, B. R., 1963, *Operator Techniques in Atomic Spectroscopy* (McGraw-Hill, New York).

Judd, B. R., 1967, *Second Quantization and Atomic Spectroscopy* (Johns Hopkins, Baltimore).

Levinson, I. B., and V. V. Vanagas, 1957, Opt. Spektrosk. **2**, 10.

Lindgren, I., and A. Rosén, 1974, in *Case Studies in Atomic Physics* (North-Holland, Amsterdam), Vol. **4**, pp. 93–196.

Mann, J. B., and W. R. Johnson, 1971, Phys. Rev. A **4**, 41.

Massot, J.-N., E. El-Baz, and J. Lafoucriere, 1967, Rev. Mod. Phys. **39**, 288.

Racah, G., 1942, Phys. Rev. **61**, 186.

Racah, B., 1942, Phys. Rev. **62**, 438.

Racah, G., 1943, Phys. Rev. **63**, 367.

Rose, M. E., 1957, *Elementary Theory of Angular Momentum* (Wiley, New York).

Rotenberg, M., R. Bivins, N. Metropolis, and J. K. Wooten, Jr., 1959, *The 3-j and 6-j Symbols* (Technology, Cambridge, Mass.).

Sandars, P. G. H., 1969, in *Brandeis Lectures in Theoretical Physics*, edited by M. Chrétien and E. Lipworth (Gordon and Breach, New York), Vol. **1**, pp. 171–216.

Sivcev, V., A. Slepcov, I. Kickin, and Z. Rudzikas, 1974, Sov. Phys.-Coll. **14**, 189.

Wigner, E. P., 1927, Z. Phys. **43**, 624.

Wigner, E. P., 1951, "On matrices which reduce Kronecker products of representations of S. R. groups" (unpublished).

Wigner, E. P., 1959, *Group Theory* (Academic, New York), p. 295.